Western&Graduate&PostdoctoralStudies

Electronic Thesis and Dissertation Repository

10-26-2022 9:00 AM

RHAMM as a biomarker and therapeutic target in triple-negative breast cancer

Britney Messam, *The University of Western Ontario*

Supervisor: Turley, Eva, *The University of Western Ontario*
A thesis submitted in partial fulfillment of the requirements for the Master of Science degree in Biochemistry
© Britney Messam 2022

Follow this and additional works at: https://ir.lib.uwo.ca/etd

⚙ Part of the Biochemistry Commons, and the Cancer Biology Commons

Recommended Citation

Abstract

Triple-negative breast cancer (TNBC) is a heterogeneous group of tumours characterized by early metastases and poor prognosis. Discovering novel biomarkers and therapeutic targets is necessary to improve TNBC patient outcomes as resistance to chemotherapy, the main therapeutic approach for TNBC, is common. In my study, RHAMM promoted proliferation of TNBC MDA-MB-231 tumour cells. RHAMM expression increased sensitivity to doxorubicin (p=0.0002) and strongly increased sensitivity to the FDA-approved MEK1/2 inhibitor trametinib (p≤0.0001). Doxorubicin and trametinib selectively killed *RHAMM*$^{+/+}$ MDA-MB-231 tumour cells grown as co-cultures with *RHAMM*$^{-/-}$ MDA-MB-231 tumour cells. *RHAMM*-loss or trametinib decreased phosphorylated ERK1/2 protein levels and promoted apoptosis through cell surface RHAMM/HA interactions. The combination of paclitaxel, a chemotherapeutic, and trametinib synergistically promoted apoptosis of the *RHAMM*$^{+/+}$ MDA-MB-231 tumour cells. Therefore, RHAMM is a candidate novel biomarker in TNBC, and its expression can be exploited for targeted therapy, which has potential clinical utility for the management of TNBC.

Keywords

Triple-negative breast cancer, targeted therapy, RHAMM, hyaluronan, tumour microenvironment, biomarker, drug response, MEK therapy

Summary for Lay Audience

Triple-negative breast cancer (TNBC) is a type of breast cancer characterized by invasive tumour growth and poor patient survival outcomes. Development of resistance to current treatments, such as doxorubicin, is common. Therefore, identifying and developing effective therapies is required to improve patient outcomes. A protein called RHAMM has been reported to be highly expressed in breast cancer and my project was therefore focused on assessing if RHAMM expression in TNBC can help identify tumour cells that are more likely to die when exposed to different treatments, such as chemotherapy. In my study, the loss of RHAMM reduced TNBC cell proliferation, in part through the regulation of a protein called ERK1/2, which is highly expressed in TNBC. RHAMM expression increased the sensitivity of TNBC cells to the chemotherapeutic drug doxorubicin and trametinib, a drug that specifically targets MEK1/2, which is a highly active protein that promotes cancer progression. Doxorubicin and trametinib selectively killed RHAMM-expressing TNBC tumour cells that were grown with TNBC tumour cells that did not express RHAMM. *RHAMM*-loss or treatment with trametinib decreased the expression of activated ERK1/2 in the TNBC tumour cells and killed the tumour cells through the cell surface interaction of RHAMM and its binding partner HA. Furthermore, the combination of trametinib and a chemotherapy agent paclitaxel killed more RHAMM-expressing TNBC tumour cells than treatment with either drug alone. My results suggest that RHAMM expression in TNBC can be used as an indicator of sensitivity to treatment and that its expression and signalling can be used for targeted therapy, which has potential clinical significance for the management of TNBC.

Acknowledgements

Table of Contents

List of Tables

List of Figures

List of Abbreviations

4',6-diamidino-2-phenylindole (DAPI)

Adriamycin + cyclophosphamide (AC)

Androgen receptor (AR)

Basal-like 1 (BS1)

Basal-like 2 (BS2)

Breast cancer 1 (BRCA1)

Breast cancer 2 (BRCA2)

c-Jun N-terminal kinase (JNK)

Cyclophosphamide + adriamycin + fluorouracil (CAF)

Cyclophosphamide + epirubicin + fluorouracil + a taxane (CEFT)

Cyclophosphamide + methotrexate + fluorouracil (CMF)

Docetaxel + adriamycin + cyclophosphamide (TAC)

Docetaxel + cyclophosphamide (TC)

Doxorubicin (DOX)

Dulbecco's Modified Eagle Medium (DMEM)

Epidermal growth factor receptor (EGFR)

Estrogen receptor (ER)

Extracellular matrix (ECM)

Extracellular signal-regulated kinase (ERK)

Gap 0 (G0)

Gap 1 (G1)

Gap 2 (G2)

High molecular weight HA (HMW-HA)

Human epidermal growth factor receptor 2 (HER2)

Hyaluronan (HA)

Immunomodulatory (IM)

Low molecular weight HA (LMW-HA)

Luminal androgen receptor (LAR)

Mammalian target of rapamycin (mTOR)

Mesenchymal (M)

Mesenchymal stem-like (MSL)

Mitogen-activated protein kinase (MAPK)

Mitosis (M)

Paclitaxel (PAC)

Phosphoinositide 3-kinase (PI3K)

Poly adenosine diphosphate ribose polymerase (PARP)

Progesterone receptor (PR)

Programmed cell death protein 1 (PD1)

Programmed death-ligand 1 (PDL1)

Receptor for hyaluronan-mediated motility (RHAMM)

Synthesis (S)

Three-dimensional (3D)

Trametinib (TRA)

Transforming growth factor beta (TGFß)

Triple-negative breast cancer (TNBC)

Tris-buffered saline (TBS)

Two-dimensional (2D)

Chapter 1

1 Introduction

1.1 Breast cancer

Breast cancer is one of the most common cancers among women. It is projected to account for approximately 1 in 4 new cancer cases in Canada in 2022[1], and be the fourth most common cancer-related death overall in Canada in 2022[2]. Breast cancer is a heterogeneous disease, broken down into multiple subtypes based on molecular, histological, and clinical characteristics[3]. Histologically, breast cancer can be categorized into *in situ* carcinomas, which refer to cancer cells that do not migrate from their primary location, or invasive carcinomas[3,4] (**Figure 1**). There are two types of *in situ* carcinomas: ductal and lobular. Ductal carcinoma *in situ* forms in milk ducks, whereas lobular carcinoma *in situ* forms in breast lobules[3,4]. Invasive carcinomas are a heterogeneous group of tumours that result from the migration of ductal and lobular cancer cells into the breast tissue and eventually into other tissues[3]. Increased importance has been placed on the molecular classification of tumours because survival outcomes and response to therapy can be predicted based on a tumours genomic and transcriptomic profile. Breast cancer tumours are currently divided into six main molecular subtypes based on estrogen receptor (ER), progesterone receptor (PR), human epidermal growth factor receptor 2 (HER2) and Ki67 gene expression: normal breast-like, HER2-enriched, luminal A, luminal B, basal-like, and claudin-low[3,5–7]. Out of all the subtypes, patients with the basal-like subtype experience the shortest overall survival rates[5,6].
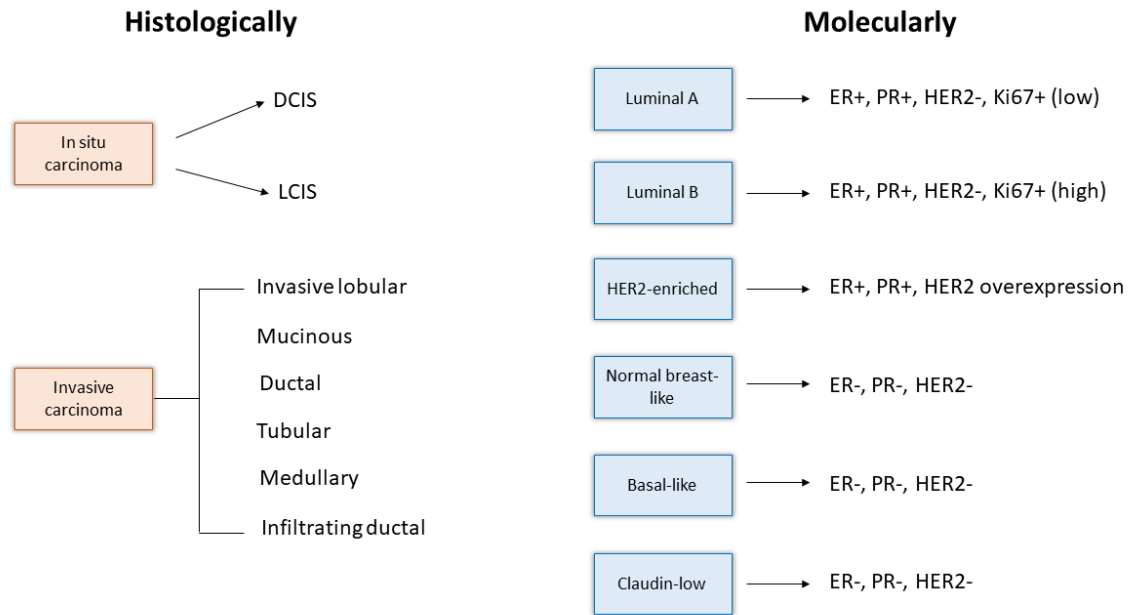
Figure 1. Histological and molecular classification of breast cancer. Histological classifications are based on morphological features of the tumour and its growth patterns. Molecular classifications are based on gene expression analysis of estrogen receptor (ER), progesterone receptor (PR), human epidermal growth factor receptor 2 (HER2) and Ki67 expression. DCIS: Ductal carcinoma *in situ*; LCIS: Lobular carcinoma *in situ*. This figure was adapted from Malhotra et al., 2010[3].

1.2 Triple-negative breast cancer

Triple-negative breast cancer (TNBC) is a heterogeneous group of tumours within the basal-like subtype that comprise 10 – 15 % of all breast cancers[7–10]. TNBC is defined by the absence of ER, PR, and HER2 expression[7,11], and is categorized into six subclassifications: basal-like 1 (BS1), basal-like 2 (BS2), immunomodulatory (IM), luminal androgen receptor (LAR), mesenchymal (M), and mesenchymal stem-like (MSL), based on gene expression profiling[12,13] (**Figure 2**). TNBC is typically highly invasive with poor prognosis[7–9]. Relative to patients with other breast cancer subtypes, TNBC patients are more likely to experience distant tumour metastases in the brain and lung tissue within the first three years after diagnosis[7,8,10,14,15]. Additionally, TNBC patients have a worse overall survival rate at every tumour stage[16] and experience higher mortality within the first five years of diagnosis[9,17] compared to patients with other breast cancer subtypes.

Immunohistochemically   **Molecularly**

| Estrogen Receptor Negative |

| Basal-like 1 | → Abnormal expression of cell cycle regulators

| Basal-like 2 | → Abnormal activation of growth factor signaling pathways

| Progesterone Receptor Negative |

| Immunomodulatory | → Highly enriched immune-cell associated genes

| Luminal Androgen Receptor | → Highly activated hormone-related signaling pathway

| Human Epidermal Growth Factor Receptor 2 Negative |

| Mesenchymal | → Highly activated cell-motility related pathways

| Mesenchymal stem-like | → High expression of stemness-related genes

Figure 2. Histological and molecular classification of triple-negative breast cancer. Triple-negative breast cancer is termed "triple-negative" because these tumours lack expression of the estrogen receptor (ER), progesterone receptor (PR), and human epidermal growth factor receptor 2 (HER2). Molecular classifications are based on gene expression profiling of TNBC tumours.

1.3 Systemic chemotherapy treatment options for TNBC

The use of biomarkers is an important strategy to determine patient response to therapy. Biomarkers can help clinicians both identify the aggressive status of a tumour and inform on how tumours will respond to chemotherapy and targeted treatments[9,18,19]. However, chemotherapy without biomarker guides remains the main systemic treatment for TNBC largely because this subtype does not express ER, PR and HER2, which are the most commonly used biomarkers for providing direction for treatment (e.g. HER2-positive breast cancer patients respond well to treatment with the HER2 inhibitor trastuzumab)[7,9]. Doxorubicin (Adriamycin) + cyclophosphamide (AC) chemotherapy or AC followed by a taxane (paclitaxel or docetaxel) chemotherapy is one of the main treatments administered to all ER-, PR- and HER2-positive breast cancer patients before their primary therapy of surgery or targeted therapy[20]. In contrast, there are no standard chemotherapy procedures for TNBC. The National Comprehensive Cancer Network recommends six different adjuvant chemotherapy regimens, which occur after the primary surgery, for TNBC based on combinations of anthracycline, cisplatin, taxane, cyclophosphamide, and fluorouracil: adriamycin + cyclophosphamide (AC), docetaxel + cyclophosphamide (TC), docetaxel + adriamycin + cyclophosphamide (TAC), cyclophosphamide + adriamycin + fluorouracil (CAF), cyclophosphamide + methotrexate + fluorouracil (CMF), or cyclophosphamide + epirubicin + fluorouracil + a taxane (CEFT). Anthracycline or anthracycline and taxane chemotherapies are an effective option for some TNBC patients who have a complete pathological response, which refers to the disappearance of all the cancer cells upon treatment[7,9,12,20]. Nevertheless, even following high sensitivity to initial chemotherapy treatments, the majority of TNBC patients experience residual disease with consequent

disease recurrence and poor overall survival outcomes[14,17,20]. Therefore, current research is focused on identifying novel molecular targets based on the subclassifications of TNBC to improve treatment outcomes.

1.4 Targeted therapy options in TNBC

Predictive markers to identify TNBC patients who will experience a pathologically complete response after chemotherapy do not exist[9]. However, identifying molecular characteristics of a tumour has proven beneficial in improving treatment response to TNBC. For example, a retrospective analysis of TNBC patients who underwent anthracycline and paclitaxel chemotherapy found that amongst the BL1, BL2, MSL and LAR TNBC subtypes, patients with the BL1 subtype had the highest complete response of 52%, followed by the MSL, LAR and BL2 subtypes, with responses of 23, 10 and 0%, respectively[21]. Multiple preclinical and clinical studies have explored the effect of targeted treatments based on TNBC subtypes. For example, the BL1 TNBC subtype is characterized by DNA repair and cell cycle regulation abnormalities, such as germline mutations in the breast cancer 2 (BRCA2) gene[13,22]. DNA repair is facilitated by multiple repair pathways, such as mismatch repair, non-homologous end joining and homologous recombination[23,24]. BRCA1 and BRCA2 are a set of genes within the DNA repair pathway important for homologous recombination after double-stranded breaks. The prevalence of germline BRCA1/2 mutations is highest in TNBC patients compared to other breast cancer subtypes[7,12,25]. Therefore, platinum salts, genotoxic drugs, or inhibitors against poly adenosine diphosphate ribose polymerase (PARP), which is important for base-excision repair, are often used against these tumours because they induce massive DNA damage and consequently promote tumour cell apoptosis[21,26]. Two phase III clinical trials, OlympiAD

and EMBRACA, were conducted to assess the overall response rates of TNBC patients with germline BRCA1/2 mutations treated with PARP inhibitors with the idea that deficits in DNA repair caused by non-functional BRCA genes make cells sensitive to further inhibition of DNA repair proteins. In the OlympiAD clinical trial, olaparib, a PARP inhibitor, increased the median progression-free survival from 4.2 to 7 months and patients had an overall response rate of 59.9% compared to a chemotherapy response rate of 28.8%[27]. In the EMBRACA clinical trial, the PARP inhibitor talazoparib increased the median progression-free survival from 5.6 to 8.6 months and patients had an overall response rate of 62.6% compared to a chemotherapy response rate of 27.2%[28]. However, significant improvements in overall survival relative to chemotherapy were not observed[27,28]. Since the clinical benefits of administering PARP inhibitors as a single-agent neoadjuvant treatment are limited[26], additional clinical trials using PARP inhibitors with DNA-damaging chemotherapy or in a neoadjuvant setting are underway and showing promise[29–31].

Androgen receptor (AR) inhibitors are commonly recommended for the treatment of LAR tumours since these tumours are driven by overexpression of AR and subsequent AR signalling[13]. Clinical studies exploring the effect of the AR inhibitors bicalutamide and enzalutamide have shown low clinical benefit rates (<30%) in AR-positive TNBC patients[32,33]. However, because LAR tumours also display high rates of phosphoinositide 3-kinase (PI3K) mutations[13,34], recent preclinical and clinical trials combining AR inhibitors with PI3K inhibitors have shown improved clinical benefit[22,35].

Growth factor receptor inhibitors, such as those inhibiting the epidermal growth factor receptor (EGFR) or the nerve growth factor receptor, are effective against BL2 tumours

because the signalling pathways associated with these growth factors are often abnormally activated[36–38]. A randomized phase II clinical trial in TNBC patients explored the effect of cetuximab, a monoclonal antibody targeting EGFR, or the combination of cetuximab and carboplatin. Response rates were only 6 and 17%, respectively[39]. In another randomized phase II clinical trial, the addition of cetuximab to metastatic TNBC patients receiving cisplatin increased the response rate from 10% to 20% and slightly increased progression-free survival from 1.5 to 3.7 months. However, the primary endpoint (overall response rate) of the study was not met[40]. Thus, despite positive experimental results, EGFR inhibitors have shown limited benefit in a clinical setting of TNBC cancer[8,9].

The IM subtype of TNBC is highly enriched with genes associated with the immune system, such as T-cell receptor genes and interferon regulatory factors[13]. Immune checkpoint inhibitors against immune markers such as programmed cell death protein 1 (PD1) and programmed death-ligand 1 (PDL1), a receptor-ligand system that mediates suppression of anti-tumour immune responses, are often administered for these tumours[13]. Clinical trials targeting PD1/PDL1 have overall response rates of less than 20%[41,42]. However, patients who respond well to treatment experience better overall survival rates[42]. More research exploring the effect of schedule dependency and combination therapies with chemotherapy agents is underway[43].

The M subtype of TNBC is defined by the activation of pathways important for migration and differentiation[13], whereas the MSL subtype is defined by high expression of stem-related genes[13]. Drugs that target migration, such as those against mammalian target of rapamycin (mTOR), are hypothesized to be effective against M tumours[44], while Src and PI3K inhibitors are hypothesized to be effective against MSL tumours[45]. In phase I study,

the response rate of TNBC patients with the M subtype treated with the mTOR inhibitors temsirolimus and everolimus was only 21%[46]. Moreover, a phase I study was conducted to explore the effect of inhibiting NOTCH signalling using a γ-secretase inhibitor, since NOTCH signalling is important for stem cell development and differentiation[47,48], and because the NOTCH pathway is upregulated in M and MSL TNBC subtypes[49]. However, most of the patients had to discontinue using the inhibitor due to disease progression and the overall response rate was low[49].

While these studies demonstrate the benefits of applying targeted therapies to improve treatment response in TNBC, they also highlight the need for additional markers to identify treatment-susceptible tumours.

1.5   The role of the RAS/RAF/MEK/ERK cascade in TNBC

Mitogen-activated protein kinase (MAPK) signalling pathways are promising therapeutic targets as they are commonly hyperactivated in many human cancers, including TNBC. MAPK pathways are grouped into four cascades based on the terminal MAPKs: extracellular signal-regulated kinase (ERK) 1/2, p38, c-Jun N-terminal kinase (JNK) and ERK5. MAPK pathways are typically composed of three to five protein kinases: MAPK kinase kinase (MAPKKK), MAPK kinase (MAPKK), MAPK, and MAPK-activated protein kinases (MAPAPK). This kinase cascade transmits extracellular signals from growth factors, ECM components, and factors released by tissue stress, including from tumours, into intracellular signals that promote cell proliferation, survival, and differentiation[50,51].

Of the four cascades, the ERK1/2 cascade is the most frequently mutated and activated pathway[52]. The ERK cascade is composed of RAS, RAF, MEK1/2, ERK1/2 and

downstream protein kinases activated by ERK[50,51]. Upon activation through dual phosphorylation at threonine and tyrosine residues by MEK1/2, ERK1/2 is translocated to the nucleus where it phosphorylates transcription factors important for cell proliferation, differentiation, motility, apoptosis, and angiogenesis[53–55] (**Figure 3**). Continual activation of the MEK/ERK cascade, usually through mutations in *RAS* or *BRAF* results in de-regulated proliferation and reduced apoptosis that is conducive to tumour development[52]. High levels of activated ERK1/2 occur in breast cancer tumour cells and correlate with lymph node metastasis[56,57]. Furthermore, in TNBC, elevated ERK1/2 expression and activation promotes metastasis[58] and is associated with lower overall, recurrence-free, and distant metastasis-free survival rates[58–60]. Inhibition of this pathway reduces tumour progression and reverts cells to a homeostatic state in experimental models[58,61,62]. Because ERK1/2 is the only substrate of MEK1/2[50,51,63] and has a strong role in promoting tumour progression, targeting the MEK/ERK cascade is an enticing and potentially advantageous approach for abrogating tumour development within TNBC.

1.6 Trametinib as a targeted therapy against the RAS/RAF/MEK/ERK cascade in TNBC

Trametinib is a highly specific, non-ATP competitive inhibitor of MEK1/2 that inhibits activation by RAF[63]. A clinical study investigating the pharmacokinetics of the combination of dabrafenib, a BRAF inhibitor, and trametinib versus dabrafenib alone in metastatic melanoma patients with BRAF[V600E,K] mutations found that the combination therapy reduced the incidence of cutaneous squamous cell carcinoma, increased the median progression-free survival and increased response rates[64]. This study and prior clinical studies showing high response to rates to trametinib[65] led to the approval of trametinib as a

combination therapy with dabrafenib to treat unresected or metastatic melanoma patients with B-Raf[V600E,K] mutations[66]. Since then, trametinib has been investigated for its anti-tumour properties with several other chemotherapy agents, such as the PI3K inhibitor BKM120[67], the BCL-2 inhibitor navitoclax[68], and the AKT inhibitor GSK2141795[69]. However, there are currently only limited clinical trials showing success with trametinib in TNBC patients. In a single-arm multi-center study exploring the effect of trametinib or trametinib in combination with the AKT inhibitor GSK2141795 in advanced TNBC, both treatment options showed little efficacy in the majority of patients[70]. Two patients who were administered trametinib alone experienced a partial response and one patient administered trametinib and GSK2141795 experienced an unconfirmed partial response[70]. These results highlight the heterogeneity in response to treatment within TNBC patients and underscore the importance of identifying biomarkers that can be used to predict positive treatment responses.

Despite some of the benefits observed with trametinib, most cancer patients experience dose-limiting toxicities, such as rashes, diarrhea, peripheral edema and central serous retinopathy[64,65,70]. Dose-limiting toxicity is a common problem with drugs that target the MEK/ERK cascade because of its wide expression profile and involvement with multiple homeostatic cellular processes[71–73]. Finding new ways to reduce these toxicities would improve the usability of this drug. Biomarkers to tumours that are sensitive to low doses of MEK inhibitory drugs is one approach to improving the use of this targeted therapy[74,75].
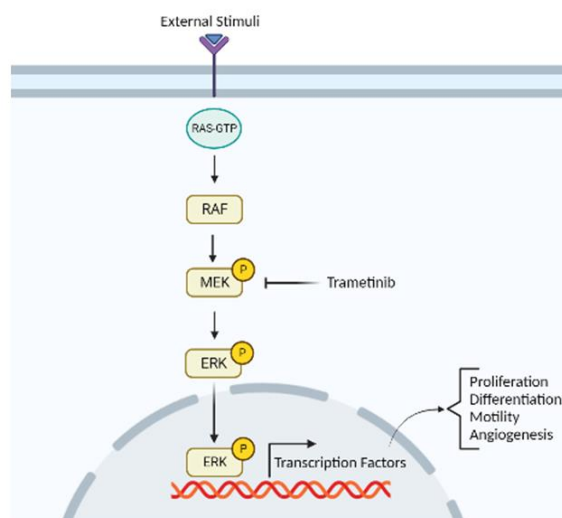
Figure 3. RAS/RAF/MEK/ERK cascade with an inhibitor of MEK. The RAS/RAF/MEK/ERK cascade is one of four cascades in the MAPK signalling pathway. When this pathway is activated by external stimuli, such as growth factors, RAS is transformed into its active form through the conversion of RAS-bound GDP to GTP. This sets off a signalling cascade where activated RAS, activates RAF, which activates MEK1/2, which activates ERK1/2. ERK1/2 goes on to activate a diverse array of substrates that play roles in promoting proliferation, differentiation, motility, and angiogenesis. Trametinib is a highly specific, non-ATP competitive inhibitor of MEK1/2. Created with Biorender.com[76]

1.7 Biology of HA and RHAMM

Tumour progression and metastasis is a multi-step process that requires key contributions from the tumour microenvironment[77]. Changes in the morphology and motile capability of the primary tumours are dependent on extracellular matrix (ECM) components such as hyaluronan (HA) and HA receptors such as the receptor for hyaluronan-mediated motility (RHAMM), which regulate signalling through ERK1/2 to control these processes[78].

HA is a glycosaminoglycan made up of repeating units of N-acetyl glucosamine and β-glucuronic acid. HA is a vital ECM component implicated in regulating both anti-tumour and pro-tumour phenotypes depending on its molecular weight. High molecular weight HA (HMW-HA) (>500 kDa) is characterized as being anti-inflammatory and anti-fibrotic and important for maintaining tissue architecture and hydration in homeostatic tissue[79–81]. In contrast, low molecular weight HA (LMW-HA) (10-250 kDa), which is produced by fragmentation of HMW-HA by hyaluronidases or reactive oxygen species[82], is a danger signal to promote pro-inflammatory responses, cell proliferation and migration[80,81,83,84]. LMW-HA, in particular, is conducive to tumour progression in breast cancer[85,86]. For example, a study exploring the prognostic potential of LMW-HA in breast cancer found that breast cancer patients expressed higher levels of serum LMW-HA than healthy women[81,87,88]. Furthermore, among breast cancer patients, higher serum LMW-HA levels were correlated with lymph node metastases[89]. In addition, invasive breast cancer cell lines produced LMW-HA to a greater extent than non-invasive cell lines[89].

RHAMM (gene name *HMMR*) is a multifunctional HA receptor that is expressed extra- and intracellularly. It is present at low concentrations in the cytoplasm of homeostatic adult tissues[81,87,88] but is highly expressed in the placenta[87,88], thymus[87,88], testes[87,88,90], and

spleen[91,92]. During tissue/cellular stress, such as during wound healing and/or inflammation, RHAMM expression increases and is exported into the microenvironment, where it interacts with various ECM components and growth factor receptors to facilitate rapid tissue repair and in diseases such as cancer during tumour progression to an invasive and metastatic state[79,93,94].

Intracellular *RHAMM* is among a set of genes that are highly expressed during the Gap 2 (G2) and mitotic (M) phases of the cell cycle[95–97], where it regulates the structure of microtubules in each mitotic phase, controls the rate of spindle assembly and mitosis and is important for establishing microtubule nucleation sites[98,99]. Localization of RHAMM to interphase and mitotic microtubules, centrosomes and the perinucleus/nucleus predicts this protein functions in genomic stability, proliferation, and gene transcription[78,98,100,101]. Extracellular RHAMM interacts with multiple different proteins, such as platelet-derived growth factor receptor[102,103], EGFR[104,105] and transforming growth factor beta (TGFß)[106,107], but its interaction with the HA receptor CD44 is required for activation of motogenic signalling cascades such as ERK1/2[78,79,108,109]. At the cell surface, RHAMM can bind to LMW-HA to initiate signals that lead to increases in cell migration, tumorigenesis, and wound repair[81,84,110].

1.8 RHAMM as a prognostic factor and biomarker in cancer

RHAMM is a marker of poor prognosis in a variety of human cancers, including breast cancer[57,111–114], multiple myeloma[115,116], oral squamous cell carcinoma[117], prostate cancer[118], colorectal cancer[119–121], and gastric cancer[122,123]. Tumour cells utilize RHAMM function to achieve metastasis because it is a key regulator of HA-mediated cell motility.

As such, RHAMM expression is often localized to cellular processes or the invading fronts of tumours. In breast cancer, high RHAMM expression is observed in the focal regions of primary tumours[57], at the stromal-epithelium interface of primary breast tumours[111], in the trabeculae of budding breast tumours[111], and at the nuclear envelope of experimental BRCA1 mutant breast cancer cells[124]. Immunohistochemical analysis of RHAMM in breast cancer cohorts indicates that RHAMM is increasingly present in the progression of *in situ* carcinoma to invasive TNBC tumours and that distinct RHAMM[high] niches occur at the invasive edge of aggressive TNBC tumours[125]. In addition, the cellular localization of RHAMM coincides with the neoplastic potential of breast cancer subtypes. In the aggressive MDA-MB-231 TNBC cell line, RHAMM is observed in the perinuclear regions of cells, whereas in the less invasive MCF7 Luminal A breast cancer cell line, RHAMM is present in the cytoplasm and on cytoskeletal structures[109].

1.9   RHAMM/ERK1/2 complexes in TNBC

In TNBC, RHAMM utilizes signal transduction through the MEK/ERK cascade to promote cell motility and proliferation[57,108,109]. Analyses of RHAMM and ERK1/2 expression in breast cancer patients found that high RHAMM expression is correlated with high expression of ERK1/2 and that these tumours are associated with a higher tumour grade[57]. The expression of cell surface RHAMM is essential for the cell surface localization of CD44[108,109], and the resulting CD44-RHAMM complex is required to sense HA and for activation as well as subcellular localization of ERK1/2 to drive high motility and invasion in invasive breast cancer cell lines such as MDA-MB-231[109] (**Figure 4**). Intracellular RHAMM binds to ERK1 to act as a scaffold that complexes ERK1/2 with MEK1 to drive

activation near substrates relevant to cell motility (e.g., cytoskeleton proteins and nuclear transcription complexes)[103,126,127] (**Figure 4**).
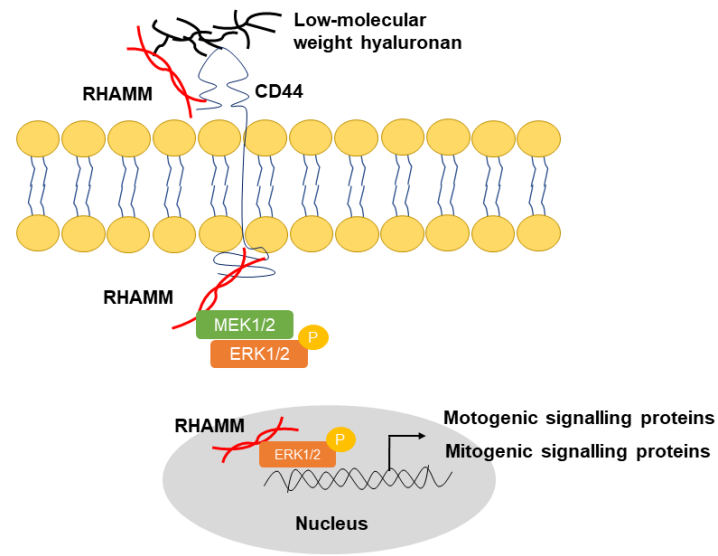
Figure 4. RHAMM is an extracellular and intracellular protein that facilitates MEK/ERK signal transduction. RHAMM binds to CD44 and LMW-HA at the cell surface to promote activation of ERK1/2. Intracellular RHAMM forms complexes with MEK1/2 and ERK1/2 to promote their activation and translocation of ERK1/2 into the nucleus to activate motogenic and mitogenic signalling proteins.

1.10 The evolution of cell culturing and therapy development: From 2D to 3D cultures

Many *in vitro* studies exploring the effect of drug sensitivity are conducted using two-dimensional (2D) cell cultures. Apart from their longstanding use in studying cell behaviour, culturing cells in 2D is a popular method because of its ease of use, cost-effectiveness, and ability to conduct high-throughput experiments. However, the results obtained from 2D cell culture experiments are not always translated or replicated in *in vivo* experiments because cells grown in 2D culture are usually flatter and more stretched than occurs *in vivo*, which changes the transcriptional and translation activity of the cells[128,129]. Three-dimensional (3D) cultures are a newer approach to improving *in vitro* to *in vivo* translatability. Currently, the most common 3D models include multicellular spheroids models, scaffold-based models, hydrogel-based models, and microfluidic chip-based models[130]. While each model uses slightly different reagents and techniques, the basis behind each is that they prevent cells from adhering to the bottom of the tissue culture plate. This promotes more cell-to-cell vs cell-to-substratum contacts and maintains the polarity and physical restraints present in the tumour microenvironment *in vivo*[131–133].

Multiple cellular processes change when cells are grown in 2D and 3D cultures. Breast cancer cells grown in 3D have been shown to form distinct spheroid morphologies, experience reduced cell viability, exhibit increased resistance to drugs and have higher cell metabolism[134]. In line with a previous study[134,135], Li *et al.*[136] found that many of the breast cancer cell lines they tested were more resistant to doxorubicin in 3D cultures than they were in 2D cultures. Similarly, in the same study, Li *et al.*[136] found that the normal epithelial cell line, MCF10A, was resistant to MEK1/2 inhibition in 3D cultures. In contrast, the

invasive breast cancer cell line MDA-MB-231 was more sensitive to MEK1/2 inhibition in 3D cultures than in 2D cultures. Taken together, these results suggest that the response of cells to changing environments can be complex and highly dependent on the cell type, culture environment and stressors. Thus, studies using both 2D and 3D cell culture techniques enable a deeper understanding of basic cellular processes and drug responses, including how these phenotypes can be influenced by factors such as cell density, protein interactions and changes in gene expression.

Following this logic, my thesis project used 2D and 3D cell cultures to examine the impact of RHAMM expression on TNBC progression.

1.11 Hypothesis and Objectives

I hypothesize that RHAMM promotes TNBC proliferation through its interaction with ERK1/2 and that RHAMM expression is a biomarker for TNBC treatment susceptibility.

The objectives of this thesis were as follows:

1. Determine the effect of RHAMM expression on proliferation and survival of MDA-MB-231 tumour cells in 2D and 3D culture models

2. Determine the sensitivity of $RHAMM^{+/+}$ and $RHAMM^{-/-}$ MDA-MB-231 TNBC cells to chemotherapy and targeted therapy in 2D cultures

3. Elucidate the role of RHAMM expression on proliferation and drug sensitivity in co-cultures of $RHAMM^{+/+}$ and $RHAMM^{-/-}$ MDA-MB-231 TNBC cells in 2D cultures

I conducted my experiments using $RHAMM^{+/+}$ and $RHAMM^{-/-}$ MDA-MB-231 cell lines kindly gifted by Drs. J. McCarthy and A. Nelson, UMN USA. The MDA-MB-231 cell line is characteristically known for its rapid growth, invasiveness and metastatic potential and

is a commonly used cell line for studying TNBC[137–139]. Molecularly, MDA-MB-231 cell lines have been classified as Basal B[140]. However, recent research shows that the cell line more closely resembles the claudin-low subtype, which is characteristic of being ER, PR and HER2-negative and having a high frequency of metaplastic differentiation[139,141]. Additionally, the MDA-MB-231 cell line exhibits the highest HA-binding levels when compared to other breast cancer cell lines[93].

Chapter 2

2 Materials and Methods

2.1 Cell Culture

The human breast cancer MDA-MB-231 cell line was purchased from American Type Culture Collection (ATCC; Manassas, USA). A *RHAMM*$^{-/-}$ MDA-MB-231 cell line was created in the lab of Dr. James B. McCarthy (University of Minnesota, Minneapolis, MN) using the CRISPR/CAS9 gene editing system. In brief, two guide RNAs targeting exon 3 and exon 6 of the *RHAMM* gene and a plasmid expressing the CAS9 enzyme with puromycin and GFP selection constructed in the lab of Dr. Brandon Moriarity (University of Minnesota, Minneapolis, MN) were co-transfected into the MDA-MB-231 cell line. Clones with a *RHAMM* deletion were detected using genomic PCR and Western Blot assays.

Cells were grown on 75 cm^2 tissue culture flasks (Sarstedt Inc., USA) and cultured in high-glucose (4.5 g/L) Dulbecco's Modified Eagle Medium (DMEM) (Wisent BioProducts, St. Burno, Quebec, Canada) supplemented with 10% (v/v) fetal bovine serum (Wisent BioProducts) and 50 μg/mL Gibco™ Penicillin-Streptomycin (Invitrogen, Life Technologies, Burlington, ON, Canada) in a 37˚C humidified atmosphere of 5% carbon dioxide. Cells were passaged every four days at 80% confluence using 0.25% Trypsin/EDTA 2.21mM in HBSS (Wisent Bioproducts).

2.2 Proliferation and drug sensitivity analysis

For 2D cultures, cells suspended in DMEM were seeded into 96-well plates (353072, Corning, USA) and incubated at 37ºC overnight. For 3D cell cultures, cells suspended in a

3:1 mixture of 4 mg/mL Corning® Matrigel® Matrix (356234, Corning, USA) and 4 mg/mL Corning™ Collagen I, High Concentration, Rat Tail (354249, Corning, USA) were seeded into 96-well plates and incubated at 37°C for 1 hour to allow the gel to solidify. After solidification, gels were supplemented with fresh DMEM and incubated at 37°C for 72 hours to allow spheroids to form. For proliferation experiments, fresh media was added 24- (2D cultures) and 72- hours (3D cultures) post-seeding and cells were grown for an additional 72 hours.

Drug sensitivity experiments were conducted using doxorubicin hydrochloride (D1515, Sigma Aldrich, USA), trametinib (GSK1120212) (S2673, SelleckChem, USA) and paclitaxel (NSC 125973) (S1150, SelleckChem, USA). 10 mM stock solutions were created by dissolving drugs in dimethyl sulfoxide. All dilutions were prepared from 10 mM stock solutions using DMEM. Drugs were added 24 hours post-seeding (2D cultures) and incubated with the cells for 72 hours. Doxorubicin was applied to triplicate wells at five different concentrations, ranging from 0.001 μM to 10 μM in a 10-fold serial dilution. Trametinib was applied to triplicate wells at eight different concentrations, ranging from 0.0002 μM to 76.125 μM in a 5-fold serial dilution. Paclitaxel was applied to triplicate wells at six different concentrations, ranging from 0.0002 μM to 0.625 μM, in a 5-fold serial dilution. Treatment wells were grown in parallel with triplicate control wells in the same culture plate.

alamarBlue™ Cell Viability (DAL1025, ThermoFisher, USA) reagent was used in 2D culture experiments to measure metabolic activity as a marker of survival and proliferation as per manufacturer protocol. In brief, 10 μL of alamarBlue™ reagent was added to each well and plates were incubated at 37°C for four hours. The reducing environment in living

cells converts resazurin, the active ingredient in alamarBlue™, to resofurin, which is highly fluorescent. Fluorescence was measured on a Biotek Synergy H4 Hybrid Plate Reader using the Gen5 software at an excitation of 560 nm and an emission of 590 nm. Metabolic activity of 3D culture experiments was quantified using the CellTiter-Glo® 3D Cell Viability (G9681, Promega, USA) reagent as per manufacturer protocol. In brief, both the plate and the CellTiter-Glo® reagent were equilibrated to room temperature for 30 minutes. CellTiter-Glo® reagent was added to the media in a 1:1 mixture and cells were mixed vigorously for 5 minutes to induce cell lysis. After the plate was allowed to settle at room temperature for 25 minutes, the luminescence signal was on a Biotek Synergy H4 Hybrid Plate Reader using the Gen5 software.

2.3   Analysis of RHAMM expression in breast cancer tissue

Breast cancer tissue sections with low, medium and high RHAMM-positive subset expression were obtained from The Human Protein Atlas (https://www.proteinatlas.org/ENSG00000072571-HMMR/pathology/breast+cancer#imid_853014). The DAB intensity of RHAMM staining within each RHAMM expression subgroup was quantified using ImageJ/Fiji (https://imagej.net/software/fiji/downloads). A Region of Interest was created by drawing a circle around the tissue section. The Region of Interest was added to the Region of Interest manager for subsequent analysis. The 4',6-diamidino-2-phenylindole (DAPI) channel was separated from the DAB channel using the "Color Deconvolution" feature in Fiji. DAB intensity of the specified Region of Interest was quantified using the "Threshold" and "Measure" features.

2.4 Analysis of GFP expression in Parental and *RHAMM*^{-/-} MDA-MB-231 co-cultures

Using 2D cultures, parental MDA-MB-231 (no GFP) and *RHAMM*^{-/-} MDA-MB-231 (GFP) cells suspended in DMEM were seeded based on the low/medium, or high *RHAMM*^{+/+} subset expression subgroups into 96-well plates and incubated at 37°C overnight. For proliferation experiments, fresh media was added 24 hours post-seeding and cells were grown for an additional 72 hours. Drug sensitivity experiments were conducted using doxorubicin hydrochloride and trametinib. Twenty-four hours post-seeding, doxorubicin and trametinib were applied to triplicate wells at five different concentrations, ranging from 0.001 μM to 10 μM in a 10-fold serial dilution and 0.0002 to 0.625 μM in a 5-fold serial dilution, respectively, and incubated with the cells for 72 hours. Treatment wells were grown in parallel with triplicate control wells in the same culture plate. GFP fluorescence was measured at an excitation of 485 nm and an emission of 512 nm on a Biotek Synergy H4 Hybrid Plate Reader using the Gen5 software.

2.5 Immunocytochemistry staining

Cells suspended in DMEM were seeded onto 12 mm coverslips (89015-725, VWR, USA) in 24-well plates (353047, Corning, USA). 24 hours later, fresh DMEM was added to the cells. Once cells reached 80% confluency, cells were washed with 1X tris buffered saline (TBS) (50 mM Tris-Cl, pH 7.5, 150 mM NaCl) for 5 minutes with gentle rocking. The cells were fixed for 10 minutes with 4% paraformaldehyde diluted in 1X TBS. After fixation, the cells were washed twice with 1X TBS for 10 minutes each with gentle rocking. The cells were permeabilized with 0.1% Triton-X (X100-5ML, Sigma Aldrich, USA) diluted in 1X TBS for 10 minutes. After permeabilization, the cells were washed twice with 1X

TBS for 10 minutes each with gentle rocking. The cells were blocked for one hour with 3% bovine serum albumin diluted in 1X TBS. After blocking, the cells were incubated with primary antibodies and stored in the dark, overnight at 4°C. The next day, the cells were washed twice with 1X TBS for 10 minutes each with gentle rocking. After the wash, the cells were incubated with secondary antibody in the dark for 1 hour (see list for antibodies used). The cells were washed twice with 1X TBS for 10 minutes each. After the wash, two drops of Prolong™ Gold Antifade Mountant with DAPI (P36931, Thermofisher Scientific, USA) were added to new slides, the coverslips were removed from the wells, inverted, and placed on top of the mountant.

2.6 Immunofluorescence staining

3D cell cultures were created by seeding cells into 24-well plates as previously described. Spheroids were grown over a seven-day growth period. At the end of the growth period, spheroids were fixed for paraffin processing using a protocol developed by Sarah Tarullo (University of Minnesota, Minneapolis, MN). In brief, the media was removed after seven days, and spheroids were fixed with 10% Neutral-Buffered Formalin for 24 hours. After fixation, 70% ethanol was added to each well. While spheroids were covered in ethanol, one vial of Epredia™ HistoGel™ Specimen Processing Gel (22-110-678, Fisher Scientific, CA) was heated for 12 seconds to liquefy the gel. Once the gel was liquified, Epredia™ Disposable Base Molds (22-050-161, Fisher Scientific, CA) were placed on ice and coated with HistoGel™. The spheroid plugs were placed on the coated moulds and additional HistoGel™ was added to submerge the spheroid plugs. Moulds were left on ice until the HistoGel™ solidified. Once solidified, the moulds were submerged in 10% NBF for further paraffin processing.

Once paraffin-embedded tissue slides were created, the slides were used for immunofluorescence assays. Tissue sections were deparaffinized in two changes of xylene for 15 minutes each. Xylene was removed by placing tissue sections in 100% ethanol for 10 minutes. Tissue sections were dehydrated in 95% and 70% ethanol for 10 minutes each. Slides were rehydrated in dH_2O and placed in 1X TBS buffer for 5 minutes each. Antigen retrieval was performed in 10 mM sodium citrate buffer (pH 6.0) and 0.1% Tween® 20 Detergent (655205, Millipore Sigma, CA) in a Panasonic microwave. Tissue sections were washed in 1X TBS for 10 minutes with gentle rocking. After the wash, tissue sections were blocked in 3% BSA diluted in 1X TBS for one hour with gentle rocking. Tissue sections were incubated with primary antibodies (see list for antibodies used) and left overnight in a tinfoil humidifier at 4°C. The next day, slides were washed in 1X TBS for 10 minutes with gentle rocking and subsequently incubated with secondary antibodies (see list for antibodies used) in a tinfoil humidifier for two hours at room temperature. Prolong™ Gold Antifade Mountant with DAPI and coverslips were placed on each tissue section following a final wash in 1X TBS for 10 minutes with gentle rocking.

Table 1. List of primary and secondary antibodies used for immunofluorescence and immunocytochemistry.

Primary Antibody	Catalogue Number	Dilution
Phospho-p44/42 MAPK (ERK1/2) (Thr202/Tyr204)	9101S, Cell Signaling, USA	1:100
p44/42 MAPK (ERK1/2)	9102S, Cell Signaling, USA	1:100
Ki-67 (8D5)	9449S, Cell Signaling, USA	1:250
Secondary Antibody	**Catalogue Number**	**Dilution**
Goat anti-Mouse IgG (H+L) Alexa Fluor™ Plus 488	A32723, ThermoFisher Scientific, USA	1:250
Goat anti-Mouse IgG (H+L) Alexa Fluor™ Plus 555	A32727, ThermoFisher Scientific, USA	1:250
Alexa Fluor™ 555 goat anti-rabbit IgG (H+L)	A11034, ThermoFisher Scientific, USA	1:250
Alexa Fluor™ 555 donkey anti-rabbit IgG (H+L)	A31572, ThermoFisher Scientific, USA	1:250

2.7 Image analysis of immunocytochemistry and immunofluorescences slides

All tissue sections were imaged on an Olympus IX81 confocal microscope using the FV10-ASW software at 40X magnification. Total fluorescence intensity of the antibodies of interest was quantified using ImageJ/Fiji. The DAPI channel was separated from the other fluorescence colours using the "Make Composite" and "Split Channels" features in Fiji. The average size of the cells was determined using the Line tool for subsequent cell counting using the "Threshold" and "Analyze Particles" features. Fluorescence of the protein of interest was quantified using the "Threshold" and "Measure" features. To specifically quantify nuclear fluorescence intensity, each analyzed particle/nuclei was added to a manager, such that only fluorescence intensity within the recorded particles was quantified.

2.8 Western Blot

Cells in DMEM were seeded into tissue culture dishes (353004, Corning, USA) and grown overnight at 37°C. 24 hours later, media alone, 0.0025 μM of trametinib, 0.025 μM of trametinib and 0.250 μM trametinib were added to each plate for an additional 72 hours. After 72 hours, cells were washed with ice-cold 1X phosphate-buffered saline (137 mM NaCl, 12 mM phosphate, 2.7 mM KCl, pH 7.4) and proteins were extracted from the cells using radioimmunoprecipitation assay buffer (150 mM NaCl, 1% Nonidet P-40, 0.1% sodium dodecyl sulphate, 0.5% sodium deoxycholate, 50 mM Tris, pH 7.4) with 1:100 Halt™ Protease & Phosphatase Inhibitor Cocktail (78440, ThermoFisher Scientific, USA). Protein lysates were incubated in a 1:3 ratio with Laemmli Sample Buffer (1610737EDU, Bio-Rad, USA) at 95°C for 5 minutes. After determining the protein concentration of each

sample using the Pierce™ BCA Protein Assay Kit (23225, ThermoFisher Scientific, USA), 20 μg of protein was loaded into wells of a Bolt™ 4-12% Bis-Tris Plus gel (NW04120BOX, ThermoFisher Scientific, USA). Protein samples were electrophoresed at 90V and transferred onto hydrophobic PVDF transfer membranes (IPVH00010, Millipore Sigma, USA) at 30V. Membranes were blocked in 5% Milk TBST (50 mM Tris-Cl, pH 7.5, 150 mM NaCl; 0.25% Tween® 20 Detergent; 5% Skim Milk Powder) overnight at 4°C. Membranes were stained for 2 hours at room temperature with gentle rocking using phosphorylated and total ERK1/2 primary antibodies diluted in 1% Milk TBST at 1:1000 dilutions. Membranes were washed with 1% Milk TBST twice for 10 minutes with gentle rocking and stained with an Anti-Rabbit IgG (H+L) HRP Conjugate (W4011, Promega, USA) for 2 hours at room temperature with gentle rocking at a 1:5000 dilution. Membranes were submerged in 1X TBST at 4°C overnight and blocked again with 5% Milk TBST the next day for one hour at room temperature with gentle rocking. Membranes were stained for GAPDH (ab37168, Abcam, UK) for 2 hours at room temperature with gentle rocking at a 1:5000 dilution. Membranes were again stained with an Anti-Rabbit IgG HRP for 2 hours at room temperature with gentle rocking at a 1:5000 dilution. Membranes were washed with 1% Milk TBST twice for 10 minutes with gentle rocking. Membranes were developed using Immobilon Forte Western HRP substrate (WBLUF0100, Sigma Aldrich, USA) and imaged using the BioRad ChemiDox™ MP Imaging system.

2.9   Cyclized RHAMM peptide mimetic

The cyclized RHAMM mimetic peptide (ETI0152) was generously donated by the lab of Dr. Len Luyt. The 14-mer cyclized peptide was derived from the alpha-helical HA-binding

domain of the RHAMM sequence. Amino acids in domain II were 'stapled' together via lactam bridges to improve bioavailability and affinity to LMW-HA.

2.10 Schedule- and Concentration-Dependent Analysis of Synergy

Drug synergy was determined using combinations of doxorubicin, trametinib and paclitaxel. *RHAMM*^{+/+} MDA-MB-231 cells suspended in DMEM were seeded into 96-well plates. Drug combinations were grouped into Lower (Doxorubicin: 0.1 μM, Trametinib: 0.005 μM, Paclitaxel: 0.025 μM), Middle (Doxorubicin: 0.250 μM, Trametinib: 0.025 μM, Paclitaxel: 0.025 μM) and Higher (Doxorubicin: 1 μM, Trametinib: 0.025 μM, Paclitaxel: 0.125 μM) based on the amount of drug added. Drug combinations were also administered at four time schedules: Drug A 4 hours after seeding, replaced with Drug B for 68 hours, Drug A 24 hours after seeding, replaced with Drug B for 48 hours, Drug A 48 hours after seeding, replaced with Drug B for 24 hours, or Drug A and Drug B simultaneously 24 hours after seeding for 72 hours, and vice versa. Cell viability was measured using the alamarBlue™. Statistical synergy was determined using methods developed by Demidenko and Miller, 2019[142]. The Bliss model of Independence was chosen to determine synergy. The Bliss Independence model assumes that if two drugs act independently, the number of surviving cells is the product of the independent killing events of the two drugs. The formula for the Bliss Independence model in the presence of a control group is as follows:

$$lnS_A + lnS_B - lnS_C - lnS_{AB} = 0$$

, where S_A is the fraction of living cells after treatment with Drug A, S_B is the fraction of living cells after treatment with Drug B, S_C is the fraction of living cells with no drug treatment that accounts for cells that naturally die, and S_{AB} is the fraction of living cells

after simultaneous treatment with Drug A and Drug B. When this equation is log-transformed, it turns into an analysis of variance (ANOVA), which can be expressed as a linear null hypothesis.

$$H_0: \mu_1 + \mu_2 - \mu_3 - \mu_0 = 0$$

. This linear null hypothesis can be tested using a test statistic T, where statistical synergy occurs when T is positive and exceeds the critical value of the t distribution.

2.11 Statistical analyses

Experimental data are presented as mean $\pm$ standard error mean (SEM), with significance detected at p-values < 0.05. Statistical differences between two means were assessed using a Welch's t-test or a Mann-Whitney test with significance set at $p \leq 0.05$. Statistical differences between three or more means were assessed using Tukey's, Sidak's or Dunnet's multiple comparison test, where significance was set at $p \leq 0.05$. Statistical significance between IC_{50} values of survival curves was calculated from non-linear regressions generated in GraphPad Prism 7.04, where significance was set at $p \leq 0.05$.

Chapter 3

3 Results

3.1 RHAMM expression increases the proliferation of MDA-MB-231 tumour cells

TNBC cells are proliferative, invasive, and often develop resistance to chemotherapy. These characteristics enable this subtype to metastasize and form colonies in distant locations such as the brain and the lungs[17]. RHAMM has been reported to be present at the invading fronts of breast tumours and proposed to play a role in the proliferation of tumour cells in that region through its interaction with ERK1/2[78,109,143]. To first determine the impact of RHAMM expression in TNBC, the proliferation of *RHAMM*^{+/+} and *RHAMM*^{-/-} MDA-MB-231 tumour cells was quantified in both 2D and 3D cell cultures. While 2D cultures offer the benefits of being low-cost and easy to manage, 3D cultures are an attractive cell culture technique as they are more representative of an *in vivo* microenvironment[144,145]. 3D cultures allow cells to form and maintain cellular contacts due to the matrix environment the cells are grown in[131,146]. This, in conjunction with various growth factors, creates a conducive environment for spheroid formation and invasion that more closely replicates *in vivo* tumour formation than in 2D cultures[131,146]. Additionally, 3D cultures allow for the comparison of drug response in different mechanical environments as previous research has shown the response of cells to drug therapy can be different between 2D and 3D cultures[136,147]. The *RHAMM*^{-/-} MDA-MB-231 cell line was created using CRISPR-CAS9 gene editing and achieved by transfecting cells with guide RNAs against exons 3 and 6 of the *RHAMM* gene and a plasmid expressing the CAS9 enzyme. The *RHAMM*^{+/+} MDA-MB-231 cell line was created by mock-transfecting the

cells to confirm that the transfection agents did not affect *RHAMM*-loss. Loss of RHAMM protein in the *RHAMM*^{-/-} MDA-MB-231 cell line was confirmed by Western Blot assays (**Figure 5A**). Metabolic activity in *RHAMM*^{+/+} and *RHAMM*^{-/-} MDA-MB-231 tumour cells was quantified as a measure of survival and proliferation, while Ki67 activation was quantified as a more specific measure of proliferation in 2D and 3D cultures as it is expressed in the active phases of the cell cycle. *RHAMM*^{+/+} MDA-MB-231 cells proliferate more rapidly in both 2D (p=0.0282) and 3D cultures (p=0.0043) compared to *RHAMM*^{-/-} counterparts, as determined by alamarBlue™ and CellTiter-Glo® assays (**Figure 5B, C, D, E**). *RHAMM*^{+/+} MDA-MB-231 tumour cells also express higher levels of Ki67 than *RHAMM*^{-/-} counterparts in both 2D culture (p=0.0005) and 3D spheroids (p=0.0003) (**Figure 6**).

RHAMM expression is important for the activation and compartmentalization of ERK1/2[103,108]. The spatial regulation of ERK1/2 by RHAMM provides cues for modulating ERK1/2-mediated migration and invasion[108]. To assess whether the increase in RHAMM-mediated cell proliferation is associated with the activation of ERK1/2, phosphorylated ERK1/2 (T202/Y204) and total ERK1/2 expression were quantified in *RHAMM*^{+/+} and *RHAMM*^{-/-} MDA-MB-231 tumour cells via immunofluorescence staining. The expression of phosphorylated ERK1/2, which is a readout of its active form, is significantly higher in *RHAMM*^{+/+} versus *RHAMM*^{-/-} 2D cells (p<0.0001) and 3D spheroids (p=0.0004), while the expression of total ERK1/2 is not significantly modified by *RHAMM*-loss (**Figure 7**). Taken together, these results show that RHAMM plays a role in promoting the proliferation of MDA-MB-231 tumour cells, and this function is associated with activation of nuclear ERK1/2.

Changes in the microenvironment can affect multiple cellular processes, including gene transcription, signal transduction, and the levels of cell proliferation and migration, and these changes have been postulated to affect how cells respond to drug therapy[129,133]. Therefore, I next investigated whether there are differences in proliferation and ERK1/2 activation between 2D and 3D cultures to determine the best culture method to implement to explore the effect of RHAMM expression on drug sensitivity.
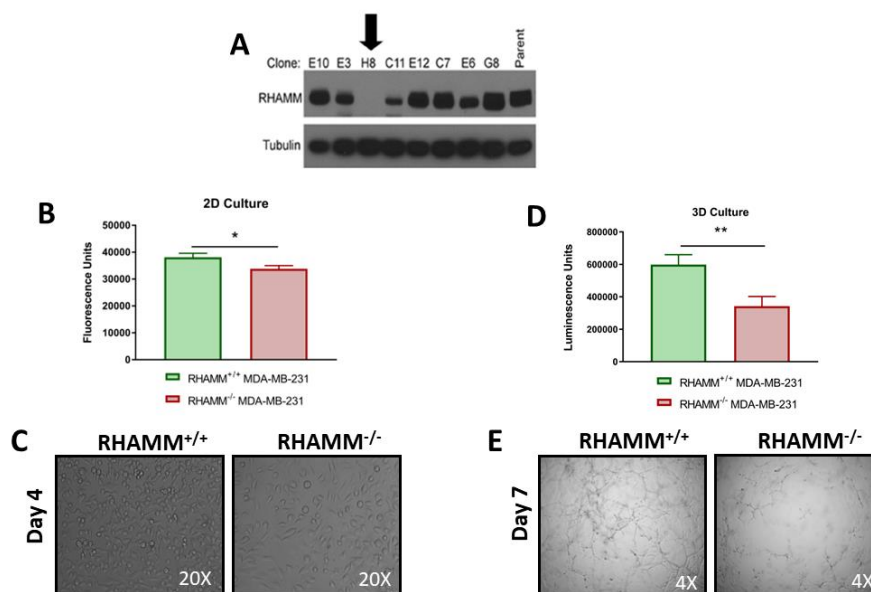
Figure 5. *RHAMM^{+/+}* **MDA-MB-231 tumour cells proliferate more rapidly than** *RHAMM^{-/-}* **MDA-MB-231 tumour cells. A)** Western blot of RHAMM knocked out of MDA-MB-231 tumour cells using CRISPR/Cas9 gene editing. Clone H8 was used as the *RHAMM^{-/-}* MDA-MB-231 cell line. **B)** *RHAMM^{+/+}* and *RHAMM^{-/-}* MDA-MB-231 tumour cells in 2D cultures were plated at 5000 cells per well in 96-well plates and grown for 96 hours. After 96 hours, cells in 2D cultures were incubated with the alamarBlue™ reagent for 4 hours, after which fluorescence was read at an excitation of 560 nm and an emission of 590 nm. Fluorescence intensity was proportional to the number of viable cells as determined by the manufacturers. Mean ± SEM, n=8, p≤0.05 (*) as determined by Welch's t-test. **C)** Representative images of 2D tumour cells at the end of the growth period taken at 20X magnification. **D)** In 3D culture, cells were embedded in a 3:1 combination of basement membrane matrix and collagen I and cells were grown for seven days. CellTiter-Glo® 3D Cell Viability reagent was added, and cells were mixed vigorously for 5 minutes before incubation with the reagent for 25 minutes, after which luminescence was recorded.

Luminescence intensity was proportional to the number of viable cells as determined by the manufactures. Mean ± SEM, n=6, p≤0.01 (**) as determined by the Mann-Whitney test. **E)** Representative images of 3D spheroids at the end of the growth period taken at 4X magnification.
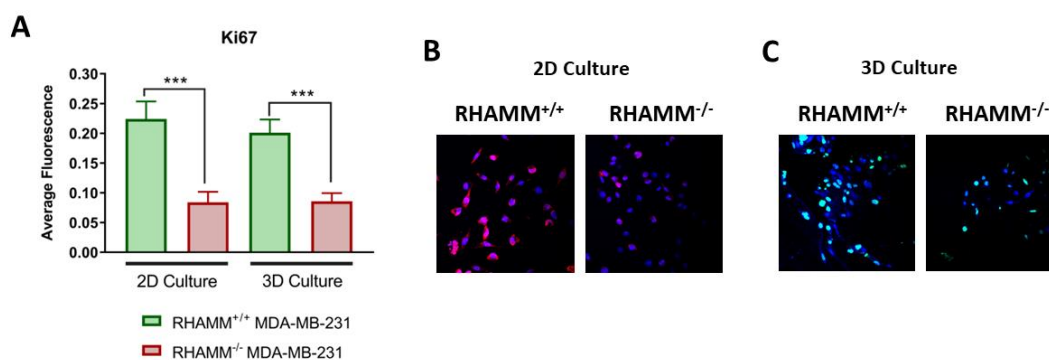
Figure 6. *RHAMM*^{+/+} **MDA-MB-231 tumour cells express higher levels of Ki67 than** *RHAMM*^{-/-} **MDA-MB-231 tumour cells. A)** Ki67 expression was quantified using ImageJ/Fiji. Mean ± SEM, $p \leq 0.001$ (***) as determined by the Welch's t-test and the Mann-Whitney test. **B)** Immunofluorescence staining of Ki67 (red) in *RHAMM*^{+/+} and *RHAMM*^{-/-} MDA-MB-231 2D cells counterstained with DAPI (blue) to visualize the nuclei. Representative images of 2D cells taken at 40X magnification. **C)** *RHAMM*^{+/+} and *RHAMM*^{-/-} MDA-MB-231 paraffin-embedded 3D spheroid sections stained with Ki67 (green) and counterstained with DAPI (blue) to visualize the nuclei. Representative images of 3D spheroids taken at 40X magnification.
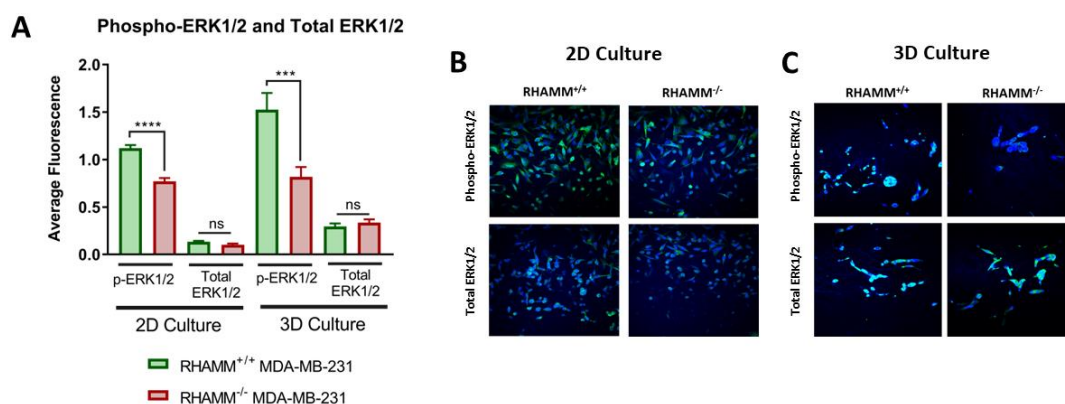
Figure 7. *RHAMM^{+/+}* **MDA-MB-231 tumour cells express higher levels of phosphorylated ERK1/2 than** *RHAMM^{-/-}* **MDA-MB-231 tumour cells. A)** Phosphorylated ERK1/2 and total ERK1/2 expression were quantified using ImageJ/Fiji. Mean ± SEM, ns = not significant, $p \leq 0.001$ (***), $p \leq 0.0001$ (****) as determined by the Welch's t-test and the Mann-Whitney test. **B)** Immunofluorescence staining of phosphorylated ERK1/2 (green) and total ERK1/2 (green) in *RHAMM^{+/+}* and *RHAMM^{-/-}* MDA-MB-231 2D cells stained counterstained with DAPI (blue) to visualize the nuclei. Representative images of 2D cells taken at 40X magnification. **C)** Immunofluorescence staining of phosphorylated ERK1/2 (green) and total ERK1/2 (green) in *RHAMM^{+/+}* and *RHAMM^{-/-}* MDA-MB-231 paraffin-embedded 3D spheroid sections counterstained with DAPI (blue) to visualize the nuclei. Representative images of 3D spheroids taken at 40X magnification.

3.2 The effect of RHAMM expression on Ki67 expression and ERK1/2 activation does not differ between 2D and 3D cultures

To determine if there are culture-specific differences in proliferation and ERK1/2 activation in *RHAMM*$^{+/+}$ and *RHAMM*$^{-/-}$ MDA-MB-231 tumour cells between 2D and 3D culture conditions, ratios of each readout, proliferation/survival, Ki67 expression, and phosphorylated ERK1/2, were compared. The effect of RHAMM expression on MDA-MB-231 tumour cell proliferation/survival is significantly larger in 3D cultures compared to 2D cultures (p=0.0026) (**Figure 8A**). In contrast, the effect of RHAMM on ERK1/2 activation and Ki67 expression is not significantly different between 2D and 3D cultures (phosphorylated ERK1/2: p=0.2837, total ERK1/2: p=0.0755, Ki67: p=0.4779) (**Figure 8B, C**). The effect of RHAMM expression on proliferation highlights important findings on the role of RHAMM in anchorage-independent vs. dependent culture conditions, which future work will address. Since there is no difference in the effect of RHAMM on Ki67 expression and ERK1/2 activation between 2D and 3D cell cultures, I next investigated the role of RHAMM on drug sensitivity using 2D cultures as it facilitates assay development and the determination of IC$_{50}$.

Chemotherapy, which primarily targets proliferating cells, is the main systemic treatment option for TNBC patients. Because *RHAMM*$^{+/+}$ MDA-MB-231 tumour cells proliferate more rapidly than *RHAMM*$^{-/-}$ MDA-MB-231 tumour cells, as detected by Ki67 expression, I explored the effect of RHAMM expression on sensitivity to chemotherapy drugs that are commonly used in TNBC to kill proliferating tumour cells.
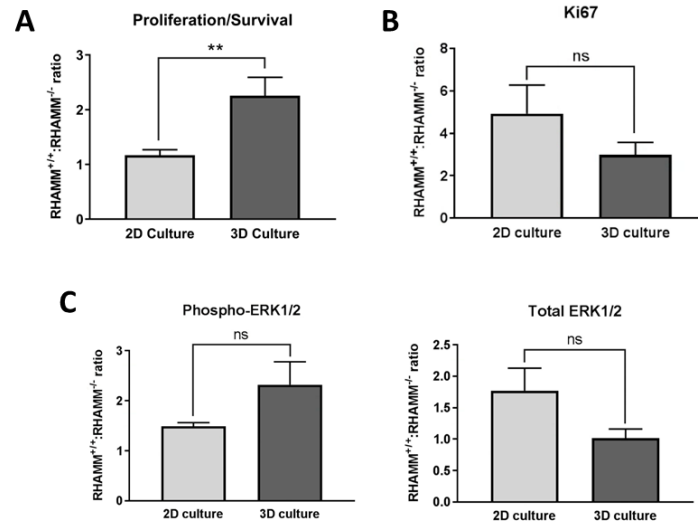
Figure 8. The effect of RHAMM expression between 2D and 3D cultures differs regarding proliferation/survival, but not to Ki67 expression or ERK1/2 activation. A ratio was created of the **A)** proliferation/survival, **B)** Ki67, **C)** phosphorylated ERK1/2 and total ERK1/2 readouts between $RHAMM^{+/+}$ and $RHAMM^{-/-}$ MDA-MB-231 cells. The magnitude of the ratio was compared between 2D and 3D cultures. Mean $\pm$ SEM; ns = not significant, $p < 0.01$ (**) as determined by the Mann-Whitney test and the Welch's t-test.

3.3 *RHAMM*^{+/+} MDA-MB-231 tumour cells are more sensitive to doxorubicin than *RHAMM*^{-/-} MDA-MB-231 tumour cells

Doxorubicin hydrochloride (Adriamycin) is commonly used in the treatment of TNBC. Doxorubicin induces DNA damage and apoptosis by several mechanisms, such as through the production of free radicals[148] and the inhibition of topoisomerase II activity[149]. Paclitaxel, which is commonly used in combination with doxorubicin, acts as a mitotic inhibitor through its stabilization of microtubules[150]. I predicted that RHAMM expression might affect sensitivity to doxorubicin and paclitaxel because RHAMM regulates proliferation, which doxorubicin indirectly inhibits through its induction of DNA damage and apoptosis, and RHAMM also associates with α- and β-tubulin to regulate microtubule dynamics, which paclitaxel abrogates[98,99,126]. To determine whether RHAMM expression promotes sensitivity to doxorubicin and paclitaxel, *RHAMM*^{+/+} and *RHAMM*^{-/-} MDA-MB-231 tumour cells were exposed to 0.001 to 10 µM of doxorubicin or 0.001 to 100 µM of paclitaxel for 72 hours. Cell viability was measured at the end of treatment using alamarBlue™. Drug sensitivity was quantified by calculating the 50% inhibitory concentration (IC_{50}) of both doxorubicin and paclitaxel. RHAMM expression significantly increases sensitivity of the MDA-MB-231 tumour cells to doxorubicin (*RHAMM*^{+/+} IC_{50}: 0.1628 µM, *RHAMM*^{-/-} IC_{50}: 0.5084 µM; p=0.0002) (**Figure 9A, C**). In contrast, and unexpectedly, RHAMM expression does not affect sensitivity to paclitaxel (*RHAMM*^{+/+} IC_{50}: 0.05451 µM, *RHAMM*^{-/-} IC_{50}: 0.05727 µM; p=0.9521) (**Figure 9B, D**). Together, these results suggest that RHAMM expression promotes sensitivity to doxorubicin in TNBC tumour cells.

RHAMM expression is often observed in heterogenous niches within tumours and the presence of RHAMM[high] subsets is associated with tumour progression, reduced survival in breast cancer and increased invasion[93,103,113,151]. To mimic this clinical context, I next investigated the effect of varying levels of RHAMM expression on proliferation and sensitivity to doxorubicin in co-cultures of *RHAMM*^{+/+} and *RHAMM*^{-/-} MDA-MB-231 tumour cells.
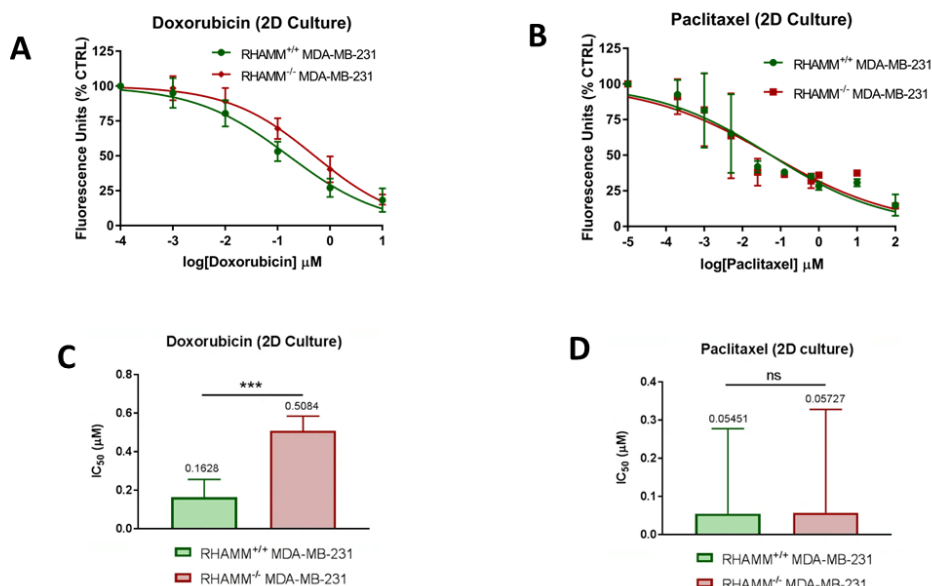
Figure 9. RHAMM expression increases sensitivity to doxorubicin, but not to paclitaxel. **A)** *RHAMM*$^{+/+}$ and *RHAMM*$^{-/-}$ MDA-MB-231 cells in 2D culture were plated at 5000 cells per well in 96-well plates and 24 hours later exposed to 0.001 to 10 µM of doxorubicin and **B)** 0.002 to 100 µM of paclitaxel for an additional 72 hours. Afterwards, cells were incubated with alamarBlue™ for 4 hours and fluorescence was read at an excitation of 560 nm and an emission of 590 nm. Fluorescence intensity was proportional to the number of viable cells as determined by the manufacturers. **C, D)** The IC$_{50}$ values were calculated from non-linear regression generated in GraphPad Prism 7.04. The numbers above each bar represent the IC$_{50}$. Mean ± SEM, n=4, ns = not significant, p≤0.001 (***).

3.4 RHAMM expression promotes proliferation and doxorubicin sensitivity in a heterogeneous environment of RHAMM[high] and RHAMM^{low} tumour cells

RHAMM expression increases with stress such as during tissue repair and in tumour microenvironments[152,153]. Within tumours, the expression of RHAMM often occurs in heterogeneous patches[57,111,125]. To determine the percentage of RHAMM present in a heterogeneous environment, RHAMM expression was quantified using immunohistochemical images of breast cancer tissue sections obtained from The Human Protein Atlas. RHAMM expression was categorized into low, medium, and high subgroups based on analyses of RHAMM expression by two independent specialists (**Figure 10A**). Breast cancer tissues with a ductal carcinoma subtype were analyzed as most TNBC tumours fall under this category[7,9]. The percentage of RHAMM-positive cells within the tissue sections was quantified from these three groups using ImageJ/Fiji. The low, medium and high subgroups exhibited 3%, 4% and 29% RHAMM positivity, respectively (**Figure 10B**). Since the difference in RHAMM positivity between the low and medium subgroup is likely based on strong, localized expression in the medium RHAMM-expressing subgroup, the low and medium subgroups were treated as one group as it is difficult to recapitulate that type of expression in 2D cell cultures. Thus, the low/medium and the high groupings and the associated RHAMM positivity percentages, 4% and 29%, respectively, were used in subsequent experiments.

To elucidate the role of *RHAMM*^{+/+} subsets on cell proliferation, co-cultures of *RHAMM*^{+/+} and *RHAMM*^{-/-} MDA-MB-231 tumour cells were created. Both cell lines were seeded together in 2D cultures in the percentages associated with the low/medium and high

subgroups (**Figure 10B**). A high *RHAMM*$^{+/+}$ MDA-MB-231 subpopulation significantly increases cell proliferation compared to *RHAMM*$^{-/-}$ monocultures (p=0.0024) (**Figure 10C**). This follows a similar trend where the *RHAMM*$^{+/+}$ MDA-MB-231 monoculture proliferation is higher than *RHAMM*$^{-/-}$ monocultures (p=0.0458) (**Figure 10C**).
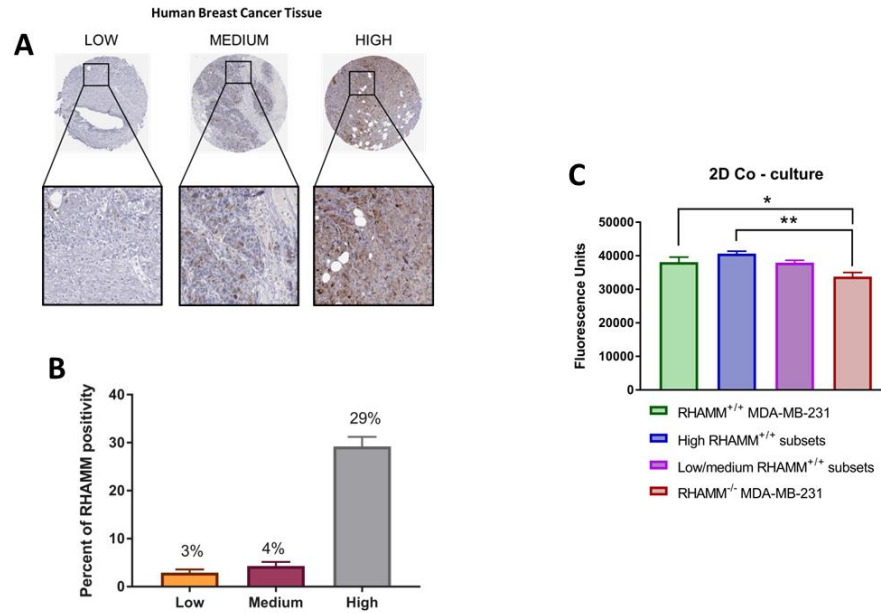
Figure 10. A high *RHAMM*⁺/⁺ subpopulation increases cell proliferation compared to *RHAMM*⁻/⁻ MDA-MB-231 monocultures. **A)** Breast cancer tissue sections were obtained from The Human Protein Atlas and separated into low (3% RHAMM-positivity), medium (4% RHAMM-positivity), and high (29% RHAMM-positivity) subgroups based on their analysis of RHAMM expression by two independent pathologists. The insets provide a closer view of the tissue. **B)** The breast cancer tissue sections were analyzed for the percentage of RHAMM expression using Image/Fiji. The numbers above each bar represent the percentage of *RHAMM*⁺/⁺ subsets. Mean ± SEM. **C)** *RHAMM*⁺/⁺ and *RHAMM*⁻/⁻ MDA-MB-231 cells were plated together in 96-well plates in 2D culture at 5000 cells per well in the proportions determined for low/medium and high RHAMM expression and cells were grown for 96 hours. After 96 hours, cells were incubated with the alamarBlue™ reagent for 4 hours and fluorescence was read at an excitation of 560 nm and an emission of 590 nm. Fluorescence intensity was proportional to the number of viable cells as

determined by the manufacturers. Mean ± SEM, n=2, $p<0.05$ (*), $p<0.01$ (**) as determined by Tukey's multiple comparison test.

RHAMM^{+/+} tumour cells occur as subsets in the tumour microenvironment[57,111,154], and these appear to be responsible for promoting breast cancer progression[125]. Since RHAMM expression promotes doxorubicin sensitivity in the MDA-MB-231 monocultures, the effect of the presence of *RHAMM*^{+/+} cell subsets on doxorubicin sensitivity was investigated using co-cultures to mimic the clinical situation. To begin to assess if RHAMM-positivity can be a biomarker for sensitivity and to determine if doxorubicin can efficiently kill *RHAMM*^{+/+}, but not *RHAMM*^{-/-}, tumour cells, *RHAMM*^{+/+} and *RHAMM*^{-/-} MDA-MB-231 tumour cells were seeded in the same proportions associated with the low/medium and high subgroups (**Figure 11A**) and treated with varying amounts of doxorubicin. *RHAMM*^{+/+}, low/medium *RHAMM*^{+/+} subsets, high *RHAMM*^{+/+} subsets and *RHAMM*^{-/-} MDA-MB-231 tumour cells were exposed to 0.001 to 10 µM of doxorubicin for 72 hours. Cell viability was quantified at the end of treatment by measuring proliferation/survival via alamarBlue™ and determining the IC_{50}. Both the low/medium and high *RHAMM*^{+/+} subsets of MDA-MB-231 tumour cells in co-cultures with *RHAMM*^{-/-} tumour cells increase sensitivity to doxorubicin (Low/Medium IC_{50}: 0.2639 µM vs. *RHAMM*^{-/-} IC_{50}: 0.5084 µM, p=0.0342; High IC_{50} = 0.2074 µM vs. *RHAMM*^{-/-} IC_{50}: 0.5084 µM, p=0.0022) compared to *RHAMM*^{-/-} monocultures (**Figure 11B, C**). Taken together, these results demonstrate that RHAMM is a potential biomarker for doxorubicin sensitivity and that the presence of *RHAMM*^{+/+} cell subsets can increase sensitivity to doxorubicin.

Since doxorubicin kills proliferating cells due to its inhibition of DNA replication, I next assessed whether doxorubicin is specifically targeting the *RHAMM*^{+/+} MDA-MB-231 tumour cells in the heterogenous environment because they proliferate more rapidly than *RHAMM*^{-/-} tumour cells.
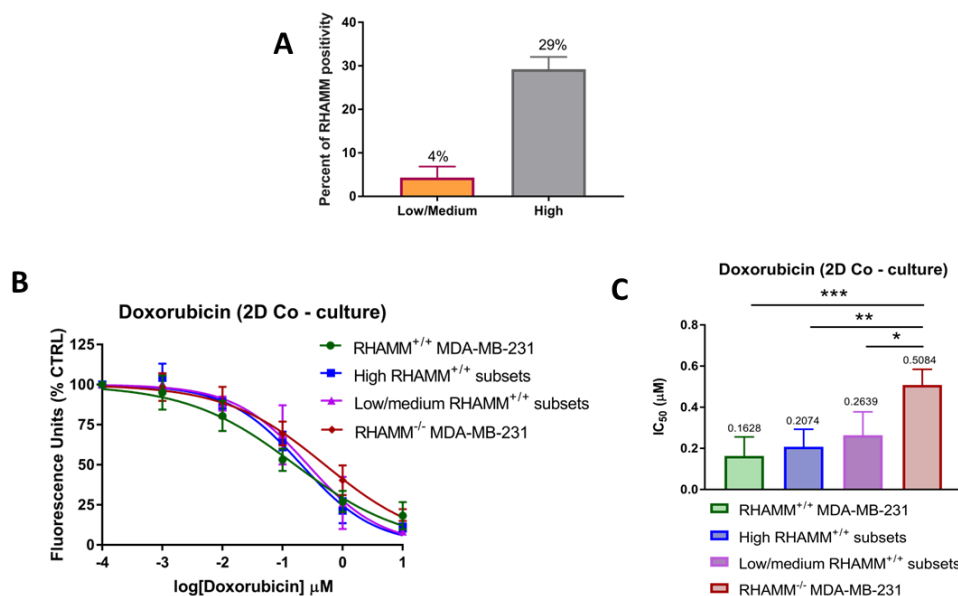
Figure 11. A low/medium and high *RHAMM*$^{+/+}$ subpopulation increases sensitivity to doxorubicin compared to monocultures of *RHAMM*$^{-/-}$ MDA-MB-231 tumour cells. A) Co-cultures were separated based on RHAMM expression into low/medium and high. The numbers above each bar represent the percentage of *RHAMM*$^{+/+}$ subsets. Mean ± SEM. **B)** *RHAMM*$^{+/+}$ and *RHAMM*$^{-/-}$ MDA-MB-231 cells were plated together in 96-well plates in 2D culture at 5000 cells per well in the proportions determined for low/medium and high RHAMM expression and 24 hours later treated with 0.001 to 10 µM of doxorubicin for an additional 72 hours. Afterwards, cells were incubated with alamarBlue™ for 4 hours and fluorescence was read at an excitation of 560 nm and an emission of 590 nm. Fluorescence intensity was proportional to the number of viable cells as determined by the manufacturers. **C)** The IC$_{50}$ values were calculated from non-linear regression generated in GraphPad Prism 7.04. The numbers above each bar represent the IC$_{50}$. Mean ± SEM, n=2, $p \leq 0.05$ (*), $p \leq 0.01$ (**), $p \leq 0.001$ (***)

3.5 Doxorubicin specifically targets *RHAMM*$^{+/+}$ MDA-MB-231 subsets in a heterogeneous environment

To create the *RHAMM*$^{-/-}$ MDA-MB-231 cell line, guide RNAs targeting RHAMM and a plasmid expressing the CAS9 enzyme with puromycin and GFP selection were co-transfected into the MDA-MB-231 cells. This allowed GFP expression to be measured to estimate the quantity of the *RHAMM*$^{-/-}$ MDA-MB-231 tumour cells in the heterogeneous population. A parental MDA-MB-231 cell line, which expresses RHAMM, but not GFP, was used as a *RHAMM*$^{+/+}$ MDA-MB-231 cell line. Low/medium RHAMM-expressing co-cultures of the parental MDA-MB-231 and *RHAMM*$^{-/-}$ MDA-MB-231 tumour cells were treated with 0.001 to 100 µM of doxorubicin for 72 hours in 2D cultures. GFP expression was measured before drug treatment and 72 hours after drug treatment to determine the percent change in GFP expression. Even though cell viability is decreasing in a concentration-dependent manner, the percent change in GFP expression upon doxorubicin treatment is not significantly different from control (**Figure 12A**). In fact, as the concentration of doxorubicin increases, the ratio between GFP expression, which is an indicator of the *RHAMM*$^{-/-}$ tumour cells, and cell viability increases (**Figure 12B**). These results suggest that the *RHAMM*$^{-/-}$ tumour cells dominate in treated cultures, and the *RHAMM*$^{+/+}$ tumour cells are increasingly killed by doxorubicin.

RHAMM$^{+/+}$ cell subsets are implicated in promoting breast cancer progression through the regulation of proliferation and motility[57,113]. As such, doxorubicin-mediated apoptosis of *RHAMM*$^{+/+}$ cell subsets has important clinical applications for the management of TNBC. Furthermore, these findings also highlight the potential use of RHAMM as a biomarker to identify aggressive tumour cell subsets.

RHAMM has previously been shown to regulate activation and subcellular localization of the MEK/ERK pathway, specifically through its ability to form MEK/ERK1/2 complexes and regulate ERK1/2 translocation[79,109]. Since ERK1/2 is the only substrate of MEK1/2[50,51,63], I hypothesized that inhibition of this pathway, by targeting MEK1/2, would preferentially affect the survival of *RHAMM*^{+/+} MDA-MB-231 tumour cells. Trametinib is a reversible and potent MEK1/2 inhibitor that is currently used to treat unresectable or metastatic melanoma[155,156]. ERK1/2 inhibition affects multiple cellular processes, such as proliferation, survival, differentiation, immune responses, and senescence[157]. Hence, trametinib is an ideal drug to investigate whether the RHAMM signalling pathway can be exploited to detect and/or increase drug sensitivity. I next verified the association between RHAMM expression and phosphorylated ERK1/2 in the MDA-MB-231 tumour cells by quantifying phosphorylated and total ERK1/2 protein levels via Western Blot, as an assessment of whether RHAMM expression predicts effective targeting of ERK1/2.
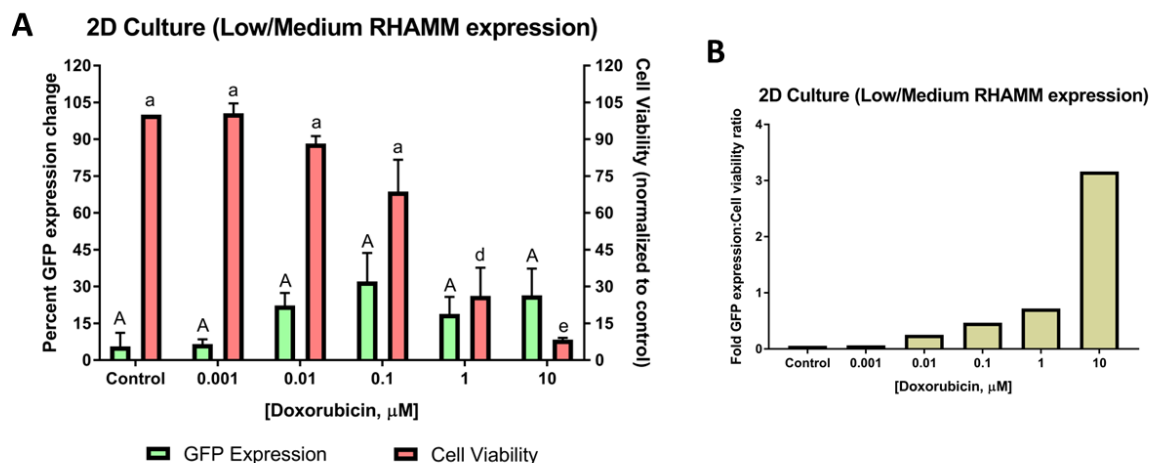
Figure 12. Doxorubicin specifically targets *RHAMM*$^{+/+}$ subsets in heterogenous co-cultures. A) *RHAMM*$^{+/+}$ and *RHAMM*$^{-/-}$ MDA-MB-231 cells were plated together in 96-well plates in 2D culture at 5000 cells per well in the proportions determined for low/medium RHAMM expression and 24 hours later treated with 0.001 to 10 µM of doxorubicin. Only the *RHAMM*$^{-/-}$ MDA-MB-231 cells are transfected with GFP, allowing for the distinction of *RHAMM*$^{-/-}$ MDA-MB-231 cells from *RHAMM*$^{+/+}$ subsets. GFP fluorescence was measured at an excitation of 485 nm and an emission of 512 nm before adding doxorubicin and 72 hours after. Mean ± SEM, n=3, upper-case letters that are the same are not significantly different from one another, lower-case letters that are the same are not significantly different from one another, d: p≤0.001 (***), e: p≤0.0001 (****) as determined by Tukey's multiple comparison test. **B)** The ratio between GFP expression and cell viability at each concentration of doxorubicin tested.

3.6   *RHAMM*^{+/+} MDA-MB-231 tumour cells express higher levels of phosphorylated ERK1/2 protein

RHAMM and ERK1/2 have experimentally been shown to directly interact to promote the transcription of key cell motility genes and regulate cytoskeletal structures[126,153]. To assess the effect of RHAMM expression on ERK activity, phosphorylated ERK1/2 (T202/Y204) and total ERK1/2 were quantified in *RHAMM*^{+/+} and *RHAMM*^{-/-} MDA-MB-231 tumour cells using Western Blot assays. The amount of phosphorylated ERK1/2 protein is significantly higher in the *RHAMM*^{+/+} MDA-MB-231 tumour cells compared to the *RHAMM*^{-/-} tumour cells (p=0.0102), while the amount of total ERK1/2 protein is not different (**Figure 13**). Since *RHAMM*^{+/+} MDA-MB-231 tumour cells exhibited increased ERK1/2 activation, I next investigated whether the interaction between RHAMM and ERK1/2 can be targeted for treatment by the MEK1/2 inhibitor trametinib.
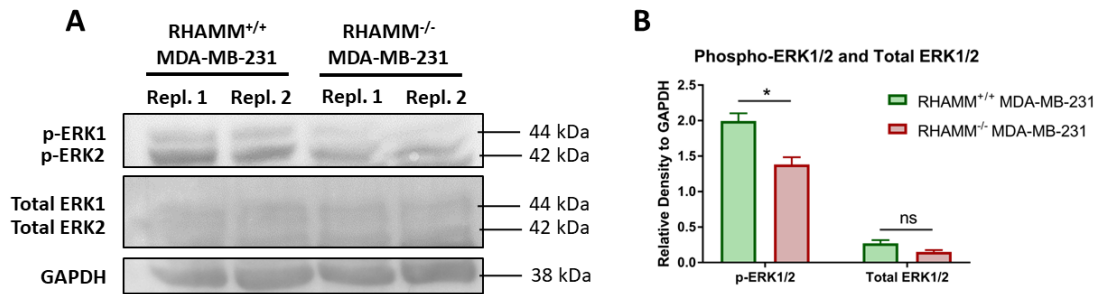
Figure 13. *RHAMM*^{+/+} **MDA-MB-231 tumour cells express higher levels of phosphorylated ERK1/2 protein than** *RHAMM*^{-/-} **MDA-MB-231 tumour cells. A)** *RHAMM*^{+/+} and *RHAMM*^{-/-} MDA-MB-231 cells were seeded into 2D culture plates and grown for 96 hours, after which, proteins were isolated from the cells and stained for phosphorylated ERK1/2 and total ERK1/2. **B)** Protein levels were quantified using ImageJ and normalized to GAPDH. Mean ± SEM, ns = not significant, p≤0.05 (*) as determined by Sidak's multiple comparison test.

3.7   *RHAMM*^{+/+} MDA-MB-231 tumour cells are more sensitive to trametinib than *RHAMM*^{-/-} comparators

To determine if there are RHAMM-dependent alterations in trametinib sensitivity, *RHAMM*^{+/+} and *RHAMM*^{-/-} MDA-MB-231 tumour cells were exposed to 0.0002 to 78.125 µM of trametinib for 72 hours. Cell viability and IC_{50} were measured at the end of treatment. RHAMM expression significantly increases the sensitivity of MDA-MB-231 tumour cells to trametinib (*RHAMM*^{+/+} IC_{50}: 0.0172 µM, *RHAMM*^{-/-} IC_{50}: 0.9618 µM; p≤0.0001) (**Figure 14**). Only a small number of clinical trials have shown success in using trametinib to treat TNBC. In the published clinical trials, few TNBC patients reached the primary endpoints of the studies since they experienced dose-limiting toxicities[70,158]. Together, these findings suggest that RHAMM may be a useful biomarker to identify patients whose tumours would respond to lower, tolerated doses of this targeted therapy.

To verify that trametinib inhibits the activation of ERK1/2 at the IC_{50}, *RHAMM*^{+/+} MDA-MB-231 cells were treated with 0.0025, 0.025 and 0.250 µM of trametinib for 72 hours. 0.0025, 0.025 and 0.25 µM of trametinib were chosen because they fall before, near and after the IC_{50} for *RHAMM*^{+/+} MDA-MB-231 tumour cells treated with the drug. Phosphorylated and total ERK1/2 protein levels in *RHAMM*^{+/+} MDA-MB-231 tumour cells after 72 hours of drug treatment were visualized and quantified using Western Blot assays. *RHAMM*^{+/+} MDA-MB-231 tumour cells exposed to 0.250 µM of trametinib express significantly lower phosphorylated ERK1/2 protein compared to control (p=0.0165), while the levels of total ERK1/2 remain unchanged (**Figure 15**).

Cell-surface RHAMM is important for promoting HA/RHAMM/CD44/ERK1/2 complexes at the cell surface that regulate ERK1/2 signalling[108,109]. Therefore, I next used a cyclized RHAMM peptide mimetic developed by Drs. Luyt and Turley[159] to determine if the RHAMM-mediated increase in trametinib sensitivity requires RHAMM/HA interactions. The cyclized RHAMM peptide mimics the HA-binding region of RHAMM and binds to LMW-HA. Therefore, it is expected to block cell surface RHAMM/HA signalling, which is a requirement for activation of the MEK/ERK cascade through RHAMM[109].
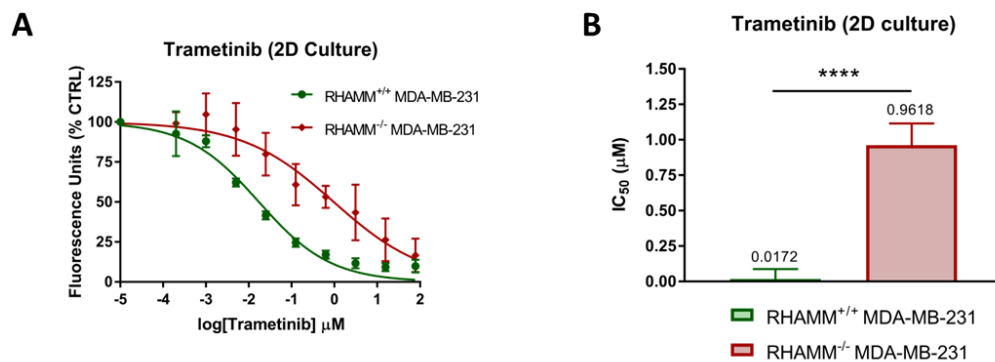
Figure 14. *RHAMM*^{+/+} **MDA-MB-231 cells are more sensitive to trametinib than** *RHAMM*^{-/-} **MDA-MB-231tumour cells. A)** *RHAMM*^{+/+} and *RHAMM*^{-/-} MDA-MB-231 cells in 2D culture were plated at 5000 cells per well in 96-well plates and 24 hours later exposed to 0.0002 to 78.125 µM of trametinib for an additional 72 hours. Afterwards, cells were incubated with alamarBlue™ for 4 hours and fluorescence was read at an excitation of 560 nm and an emission of 590 nm. Fluorescence intensity was proportional to the number of viable cells as determined by the manufacturers. **B)** The IC_{50} values were calculated from non-linear regression generated in GraphPad Prism 7.04. The numbers above each bar represent the IC_{50}. Mean $\pm$ SEM, n=3, $p \leq 0.0001$ (****).
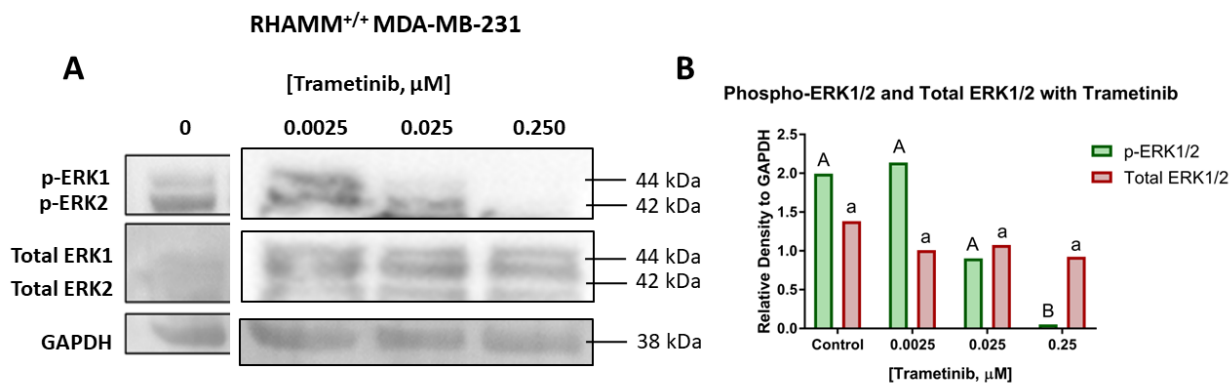
Figure 15. *RHAMM*^{+/+} **MDA-MB-231 tumour cells express lower phosphorylated ERK1/2 protein in response to trametinib. A)** *RHAMM*^{+/+} MDA-MB-231 cells were seeded into 2D culture plates and 24 hours later treated with 0.0025, 0.025 and 0.250 µM of trametinib for 72 hours. After 72 hours, proteins were isolated from the cells and stained for phosphorylated ERK1/2 and total ERK1/2. **B)** Protein levels were quantified using ImageJ and normalized to GAPDH. Mean ± SEM, upper-case letters that are the same are not significantly different from one another, lower-case letters that are the same are not significantly different from one another, B: $p \leq 0.05$ (*), as determined by Dunnett's multiple comparison test.

3.8 Sensitivity to trametinib is facilitated through cell surface RHAMM/HA interactions

To elucidate whether the increase in trametinib sensitivity is facilitated through interactions with HA at the cell surface, the sensitivity of the *RHAMM*$^{+/+}$ MDA-MB-231 tumour cells to trametinib in the presence of a cyclized peptide that blocks RHAMM/HA interactions at the cell surface was assessed. *RHAMM*$^{+/+}$ MDA-MB-231 tumour cells were exposed to a combination of 0.0025, 0.025 and 0.25 µM of trametinib and 1, 10 and 20 µM of the cyclized peptide for 72 hours. Cell viability was measured at the end of this treatment. While exposure of *RHAMM*$^{+/+}$ MDA-MB-231 tumour cells to 0.0025 µM of trametinib significantly decreases cell viability compared to control (p=0.0021), the addition of 1, 10 or 20 µM of the cyclized peptide with 0.0025 µM of trametinib increases cell viability such that it is not significantly different compared to control (**Figure 16A, B, C**). Furthermore, the addition of 1 µM of the cyclized peptide with 0.0025 µM of trametinib significantly increases cell viability compared to 0.0025 µM of trametinib alone (**Figure 16A**). The cyclized peptide thus induces a response to trametinib that is similar to *RHAMM*$^{-/-}$ MDA-MB-231 tumour cells. Together, the results suggest that trametinib sensitivity is facilitated through cell surface RHAMM/HA interactions.

Because the *RHAMM*$^{+/+}$ MDA-MB-231 monocultures are highly sensitive to targeted therapy via trametinib compared to the *RHAMM*$^{-/-}$ MDA-MB-231 monocultures, I next employed co-cultures of *RHAMM*$^{+/+}$ and *RHAMM*$^{-/-}$ MDA-MB-231 to determine whether the *RHAMM*$^{+/+}$ cell subsets can promote sensitivity to trametinib in a more clinically relevant model.
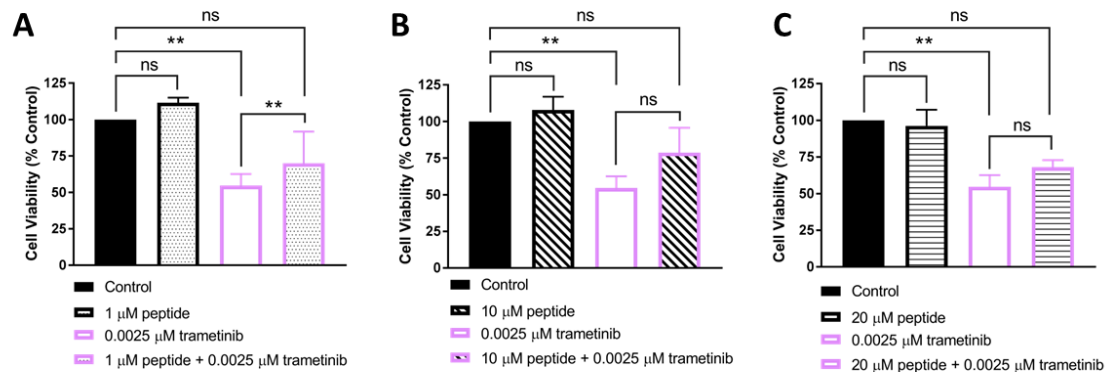
Figure 16. Trametinib sensitivity in *RHAMM*^{+/+} MDA-MB-231 tumour cells may be facilitated through cell surface RHAMM/HA interactions. *RHAMM*^{+/+} MDA-MB-231 cells were plated at 5000 cells per well in 96-well plates and 24 hours later treated with **A)** 1, **B)** 10, and **C)** 20 µM of cyclized peptide alone, 0.0025 µM of trametinib alone or combinations of cyclized peptide and trametinib for 72 hours. After 72 hours, cells were incubated with the alamarBlue™ reagent for 4 hours, after which fluorescence was read at an excitation of 560 nm and an emission of 590 nm. Mean ± SEM, n=2, ns = not significant, p≤0.01 (**) as determined by Tukey's multiple comparisons test.

3.9 RHAMM expression promotes trametinib sensitivity in co-cultures of *RHAMM*^{+/+} and *RHAMM*^{-/-} MDA-MB-231 tumour cells

To assess if *RHAMM*^{+/+} subsets generate trametinib sensitivity in *RHAMM*^{-/-} cultures, *RHAMM*^{+/+} and *RHAMM*^{-/-} MDA-MB-231 tumour cells were seeded in the proportions associated with the low/medium (4% RHAMM positivity) and high (29% RHAMM positivity) subgroups (**Figure 17A**) and treated with 0.0002 to 0.625 µM of trametinib for 72 hours. Cell viability was measured at the end of treatment and drug sensitivity was assessed by determining the IC_{50}. The low/medium and high *RHAMM*^{+/+} subsets of MDA-MB-231 tumour cells in co-cultures with *RHAMM*^{-/-} tumour cells increase sensitivity to trametinib (Low/Medium IC_{50}: 0.1579 µM vs. *RHAMM*^{-/-} IC_{50}: 0.9618 µM, p=0.0130; High IC_{50} = 0.07125 µM vs. *RHAMM*^{-/-} IC_{50}: 0.9618 µM, p=0.0004) compared to *RHAMM*^{-/-} monocultures (**Figure 17B, C**). The sensitivity of both subgroups to trametinib is significantly less than the *RHAMM*^{+/+} monocultures (*RHAMM*^{+/+} IC_{50}: 0.0172 µM vs Low/Medium IC_{50}: 0.1579 µM, p<0.0001; *RHAMM*^{+/+} IC_{50}: 0.0172 µM vs High IC_{50}: 0.07125 µM, p<0.0004) (**Figure 17B, C**). Because the co-cultures do not promote an IC_{50} as low as the pure cultures of *RHAMM*^{+/+} MDA-MB-231 tumour cells, the results indicate that the effect of trametinib is highly dependent on the levels of RHAMM expression, where high RHAMM expression is predictive of high trametinib sensitivity. Taken together, these results suggest that the presence of *RHAMM*^{+/+} subsets can promote sensitivity to trametinib. This has potential clinical significance as it provides a rationale for using RHAMM as a biomarker for trametinib sensitivity.

To elucidate whether RHAMM can be therapeutically targeted in TNBC, I next used co-cultures of *RHAMM*$^{+/+}$ and *RHAMM*$^{-/-}$ MDA-MB-231 tumour cells, that more closely approximate clinical tumours, to investigate whether trametinib can specifically induce apoptosis of the *RHAMM*$^{+/+}$ subsets.
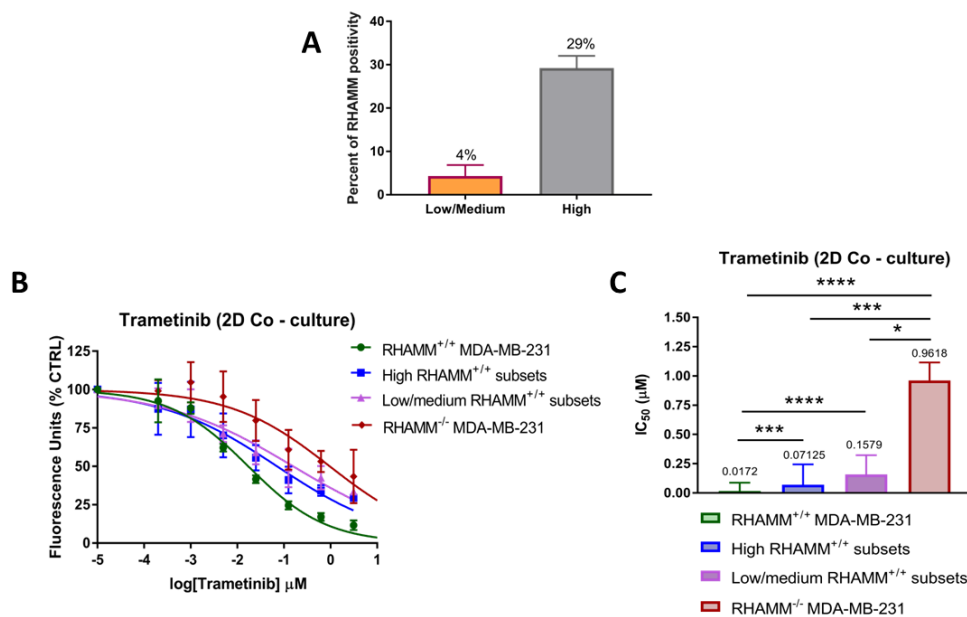
Figure 17. A low/medium and high *RHAMM*$^{+/+}$ subpopulation increases sensitivity to trametinib compared to monocultures of *RHAMM*$^{-/-}$ tumour cells. A) Co-cultures were separated based on RHAMM expression into low/medium and high. The numbers above each bar represent the percentage of *RHAMM*$^{+/+}$ subsets. Mean ± SEM. **B)** *RHAMM*$^{+/+}$ and *RHAMM*$^{-/-}$ MDA-MB-231 cells were plated together in 96-well plates in 2D culture at 5000 cells per well in the proportions determined for low/medium and high RHAMM expression and 24 hours later treated with 0.0002 to 3.125 µM of trametinib for an additional 72 hours. Afterwards, cells were incubated with alamarBlue™ for 4 hours and fluorescence was read at an excitation of 560 nm and an emission of 590 nm. Fluorescence intensity was proportional to the number of viable cells as determined by the manufacturers. **C)** The IC$_{50}$ values were calculated from non-linear regression generated in GraphPad Prism 7.04. The numbers above each bar represent the IC$_{50}$. Mean ± SEM, n=2, $p \le 0.05$ (*), $p \le 0.001$ (***), $p \le 0.0001$ (****).

3.10 Trametinib specifically targets *RHAMM*$^{+/+}$ MDA-MB-231 subsets in co-cultures

To explore the potential clinical significance of RHAMM as a therapeutic target, low/medium RHAMM-expressing co-cultures made up of parental (GFP-negative) and *RHAMM*$^{-/-}$ (GFP-positive) MDA-MB-231 tumour cells were treated with 0.0002 to 0.625 µM of trametinib for 72 hours. GFP expression was quantified 24 hours after seeding and after 72 hours of exposure to trametinib to determine the percent change in GFP expression caused by trametinib. Cell viability significantly decreases at high concentrations of trametinib, but the percent change in GFP expression does not change compared to control (**Figure 18A**). Unlike with doxorubicin where the ratio between GFP expression and cell viability increased as the concentration of doxorubicin increased, the ratio between GFP expression and cell viability in response to trametinib is the highest between 0.0002 and 0.025 µM, meaning that the *RHAMM*$^{-/-}$ MDA-MB-231 tumour cells die at higher concentrations of trametinib (**Figure 18B**). These results suggest that the dose-limiting toxicities observed with trametinib may be due to apoptosis of homeostatic tissue, which does not seem to occur with doxorubicin. Collectively, these results suggest that RHAMM is a biomarker of trametinib sensitivity in TNBC cells and that trametinib can induce apoptosis of the *RHAMM*$^{+/+}$ subsets at lower, tolerated doses, which has clinical utility.

The use of biomarkers in TNBC may enhance treatment efficacy in the absence of known targetable receptors due to the ability of biomarkers to highlight susceptible tumour populations. Combination therapies combining chemotherapy drugs with drugs that target aberrant pathways are often administered to reduce drug resistance and improve drug efficacy compared to monotherapies[74,160]. However, the clinical advancement of these

combination therapies has been hindered by a lack of predictive markers of sensitivity, including in TNBC[12,52]. Therefore, I next explored whether the presence of RHAMM in the MDA-MB-231 tumour cells can indicate sensitivity to a combination of chemotherapy, using doxorubicin or paclitaxel, and targeted therapy, using trametinib.
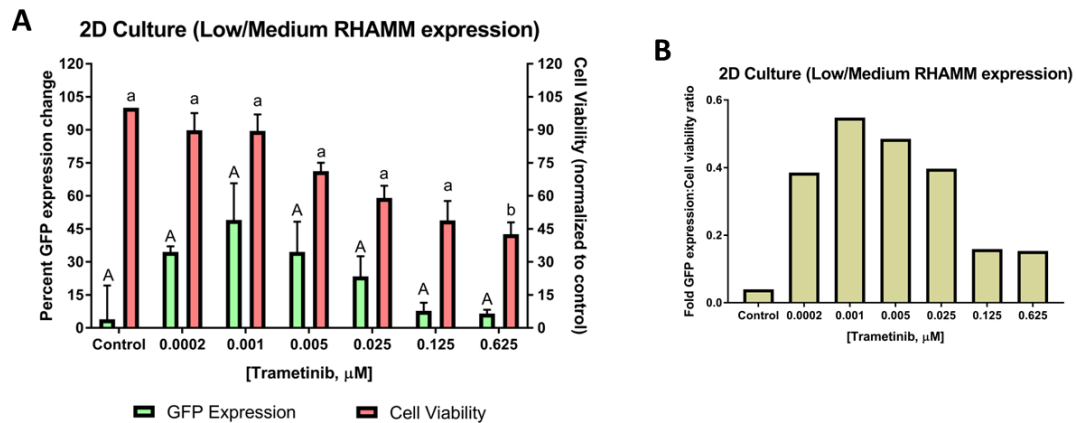
Figure 18. *RHAMM*^{+/+} **subsets are specifically targeted by low concentrations of trametinib in heterogenous co-cultures**. **A)** *RHAMM*^{+/+} and *RHAMM*^{-/-} MDA-MB-231 cells were plated together in 96-well plates in 2D culture at 5000 cells per well in the proportions determined for low/medium RHAMM expression and 24 hours later treated with 0.0002 to 0.625 µM of trametinib. Only the *RHAMM*^{-/-} MDA-MB-231 cells are transfected with GFP, allowing for the distinction of *RHAMM*^{-/-} MDA-MB-231 cells from *RHAMM*^{+/+} subsets. GFP fluorescence was measured at an excitation of 485 nm and an emission of 512 nm before adding doxorubicin and 72 hours after. Mean ± SEM, n=3, upper-case letters that are the same are not significantly different from one another, lower-case letters that are the same are not significantly different from one another, b: p≤0.05 (***) as determined by Tukey's multiple comparisons test. **B)** The ratio between GFP expression and cell viability at each concentration of trametinib tested.

3.11 The combination of doxorubicin and trametinib act independently in *RHAMM*$^{+/+}$ MDA-MB-231 cells depending on the concentration and schedule

The effect of a drug combination can be categorized as being synergistic, independent, or antagonistic. Synergism occurs when two drugs together produce an effect, such as cell death, greater than either drug alone. Independence occurs when two drugs work independently and produce an effect equal to either drug alone. Antagonism occurs when two drugs together produce an effect that is worse than either drug alone.

To determine if RHAMM expression can promote synergy between doxorubicin, which targets rapidly dividing cells, and trametinib, which targets the MEK/ERK pathway and multiple cell functions, *RHAMM*$^{+/+}$ MDA-MB-231 tumour cells were exposed to various combinations of doxorubicin and trametinib in a concentration- and time-dependent manner then cell viability was measured at the end of the treatment. As previously determined, the IC$_{50}$ of *RHAMM*$^{+/+}$ and *RHAMM*$^{-/-}$ MDA-MB-231 tumour cells treated with doxorubicin and trametinib is 0.1628 and 0.5084 µM and 0.0172 and 0.9618 µM, respectively. Therefore, 0.1, 0.250 and 1 µM of doxorubicin and 0.005 and 0.025 µM of trametinib were chosen as they are near the recorded IC$_{50}$s. Drug pairs were categorized into three groups, LOWER ([Doxorubicin] = 0.1 µM, [Trametinib] = 0.005 µM), MIDDLE ([Doxorubicin] = 0.250 µM, [Trametinib] = 0.025 µM) and HIGHER ([Doxorubicin] = 1 µM, [Trametinib] = 0.025 µM) based on the strengths of the concentrations. In addition, the drug pair was administered on a sequential- or simultaneous-based schedule that was composed of either treatment with Drug A for 4, 24 or 48 hours, followed by replacement with Drug B for 68, 48 or 24 hours, respectively, and vice versa. Simultaneous drug

administration is limited by the possibility that one drug may inhibit the function of the other. Sequential treatments provide the opportunity for each drug to function to its full capacity before its removal. Out of the 21 possible combinations of doxorubicin and trametinib, 9 act independently, and 12 act antagonistically (**Table 2**). Half of the antagonist combinations occur with doxorubicin at 0.250 µM and trametinib at 0.025 µM, regardless of the administration schedule (**Table 2**). Taken together, these results indicate that while not every combination was antagonistic, there was no synergy present between doxorubicin and trametinib in the *RHAMM*$^{+/+}$ MDA-MB-231 tumour cells. Therefore, I next investigated the synergistic potential of paclitaxel and trametinib since RHAMM regulates microtubule dynamics and RHAMM expression was a strong indicator of trametinib sensitivity.

Table 2. The combination of doxorubicin and trametinib in *RHAMM*^{+/+} MDA-MB-231 tumour cells is antagonistic or independent depending on the schedule and concentration.

					Doxorubicin and Trametinib		
DOX[a] Conc.	TRA[b] Conc.	Label	Time for DOX	Time for TRA	Fold Synergy	p-value	Interpretation
0.1	0.005	LOWER	4	68	1.318	0.0357	Independent[d]
0.1	0.005	LOWER	24	48	1.242	0.1427	Antagonistic[c]
0.1	0.005	LOWER	48	24	1.014	0.9111	Independent
0.1	0.005	LOWER	68	4	0.889	0.4255	Antagonistic
0.1	0.005	LOWER	48	24	0.704	0.0205	Antagonistic
0.1	0.005	LOWER	24	48	0.966	0.8462	Independent
0.1	0.005	LOWER	72		0.732	0.1725	Antagonistic
0.25	0.025	MIDDLE	4	68	0.96	0.8661	Antagonistic
0.25	0.025	MIDDLE	24	48	0.669	0.0976	Antagonistic
0.25	0.025	MIDDLE	48	24	0.555	0.0120	Antagonistic

0.25	0.025	MIDDLE	68	4	0.668	0.0660	Antagonistic
0.25	0.025	MIDDLE	48	24	0.619	0.0663	Antagonistic
0.25	0.025	MIDDLE	24	48	0.834	0.6096	Independent
0.25	0.025	MIDDLE	72		0.727	0.2768	Antagonistic
1	0.025	HIGHER	4	68	1.205	0.3709	Antagonistic
1	0.025	HIGHER	24	48	0.755	0.1856	Independent
1	0.025	HIGHER	48	24	0.608	0.0256	Independent
1	0.025	HIGHER	68	4	0.634	0.0399	Independent
1	0.025	HIGHER	48	24	0.669	0.0785	Antagonistic
1	0.025	HIGHER	24	48	1.161	0.5703	Independent
1	0.025	HIGHER	72		0.86	0.5601	Independent

[a]DOX = Doxorubicin

[b]TRA = Trametinib

[c]Antagonism = two drugs in combination produce effects worse than each drug alone

[d]Independent = two drugs in combination produce effects similar to each drug alone

[e]Synergism = two drugs in combination produce effects greater than each drug alone

3.12 The combination of 0.025 µM paclitaxel for 4 hours, replaced by 0.005 µM trametinib for 68 hours is synergistic in *RHAMM*$^{+/+}$ MDA-MB-231 cells

Paclitaxel induced a similar level of apoptosis in the *RHAMM*$^{+/+}$ and *RHAMM*$^{-/-}$ MDA-MB-231 tumour cells, indicating that the MDA-MB-231 tumour cells are sensitive to paclitaxel and its effect on microtubule stability, but this does not depend upon RHAMM expression. To determine if RHAMM expression can promote synergy between paclitaxel, which stabilizes microtubules, and trametinib, which reduced survival of *RHAMM*$^{+/+}$ MDA-MB-231 tumour cells, *RHAMM*$^{+/+}$ MDA-MB-231 tumour cells were treated with various combinations of paclitaxel and trametinib and cell viability was measured at the end of the treatment. Drug pairs were categorized into three groups, LOWER ([Paclitaxel] = 0.025 µM, [Trametinib] = 0.005 µM), MIDDLE ([Paclitaxel] = 0.025 µM, [Trametinib] = 0.025 µM) and HIGHER ([Paclitaxel] = 0.125 µM, [Trametinib] = 0.025 µM). Out of the 21 possible combinations, 16 are independent, 4 are antagonistic and 1 is synergistic (**Table 3**). Synergism occurs at the lower concentration range when the MDA-MB-231 tumour cells are treated with 0.025 µM of paclitaxel for four hours, replaced by 0.005 µM of trametinib for 68 hours (p=0.0357), which is a concentration of trametinib that specifically killed *RHAMM*$^{+/+}$ tumour cells (**Table 3**). Since both drugs target cellular structures and proteins that interact with RHAMM to promote proliferation, these results highlight the ability of the RHAMM signalling pathway to be specifically targeted for enhanced sensitivity to therapy.

Table 3. Synergy in *RHAMM*^{+/+} MDA-MB-231 tumour cells treated with paclitaxel and trametinib is schedule- and concentration-dependent.

PAC[a] Conc.	TRA[b] Conc.	Label	Time for PAC	Time for TRA	Fold Synergy	p-value	Interpretation
0.025	0.005	LOWER	4	68	1.318	0.0357	Synergistic[e]
0.025	0.005	LOWER	24	48	1.242	0.1427	Independent[d]
0.025	0.005	LOWER	48	24	1.014	0.9111	Independent
0.025	0.005	LOWER	68	4	0.889	0.4255	Independent
0.025	0.005	LOWER	48	24	0.704	0.0205	Antagonistic[c]
0.025	0.005	LOWER	24	48	0.966	0.8462	Independent
0.025	0.005	LOWER	72		0.732	0.1725	Independent
0.025	0.025	MIDDLE	4	68	0.96	0.8661	Independent
0.025	0.025	MIDDLE	24	48	0.669	0.0976	Independent
0.025	0.025	MIDDLE	48	24	0.555	0.0120	Antagonistic
0.025	0.025	MIDDLE	68	4	0.668	0.0660	Independent

0.025	0.025	MIDDLE	48	24	0.619	0.0663	Independent
0.025	0.025	MIDDLE	24	48	0.834	0.6096	Independent
0.025	0.025	MIDDLE	72		0.727	0.2768	Independent
0.125	0.025	HIGHER	4	68	1.205	0.3709	Independent
0.125	0.025	HIGHER	24	48	0.755	0.1856	Independent
0.125	0.025	HIGHER	48	24	0.608	0.0256	Antagonistic
0.125	0.025	HIGHER	68	4	0.634	0.0399	Antagonistic
0.125	0.025	HIGHER	48	24	0.669	0.0785	Independent
0.125	0.025	HIGHER	24	48	1.161	0.5703	Independent
0.125	0.025	HIGHER	72		0.86	0.5601	Independent

[a]PAC = Paclitaxel

[b]TRA = Trametinib

[c]Antagonism = two drugs in combination produce effects worse than each drug alone

[d]Independent = two drugs in combination produce effects similar to each drug alone

[e]Synergism = two drugs in combination produce effects greater than each drug alone

Chapter 4

4   Discussion

Identifying and developing targeted treatments for TNBC remains an ongoing challenge as TNBC patients lack ER, PR and HER2 expression required for current endocrine therapies[7,8,11]. Traditional chemotherapy without biomarker guides remains the main therapeutic approach for this subgroup of patients[7,12,161]. Thus, the discovery of novel biomarkers and therapeutic targets is required to improve patient outcomes.

4.1   RHAMM regulates the proliferation of MDA-MB-231 tumour cells and nuclear trafficking of ERK1/2

To begin to assess whether RHAMM regulates TNBC progression, I investigated the effect of RHAMM expression on cell proliferation/survival and ERK1/2 activation. Cell proliferation is dependent on the ability of cells to initiate and progress through an exquisitely controlled cell cycle[162]. The cell cycle is separated into four distinct phases, Gap 0 (G0)/Gap 1 (G1), Synthesis (S), G2, and M, that are tightly regulated to ensure proper cell division[162]. RHAMM is highly expressed in the G2/M phase of the cell cycle[97,99,163] and regulated and balanced expression of RHAMM is important for proper cell cycle progression[164]. For example, inhibition of RHAMM causes an accumulation of cells stalled in G2 and the metaphase portion of the mitotic cycle[99,165]. Moreover, interfering with RHAMM/HA interactions suppresses the synthesis of Cdc2 and Cyclin B1, which are required for entry into mitosis[165]. In my study, RHAMM expression promoted proliferation of MDA-MB-231 tumour cells in both 2D and 3D cultures, which corresponds with prior research in this lab showing that RHAMM expression promotes the proliferation of MDA-MB-231 tumour cells in 2D culture[166]. Moreover, Ki67 was expressed to a higher extent in

the *RHAMM*^{+/+} MDA-MB-231 tumour cells when compared to the *RHAMM*^{-/-} MDA-MB-231 tumour cells in both 2D and 3D cultures, predicting that RHAMM promotes cell proliferation through its ability to facilitate progression through the cell cycle as Ki67 is present during the active phases of the cell cycle, including the G1, S, G2 and M phases[167].

Dynamic instability is important for facilitating cell division in the cell cycle as cells rely on the constant growth and shrinkage of microtubules to accurately segregate their DNA[168,169]. ERK1/2 kinases have been linked to mechanisms by which RHAMM regulates microtubule stability. For example, Tolg *et al.*[126] found that RHAMM binds directly and indirectly to MEK1 and ERK1/2, allowing them to bind to tubulin and phosphorylate microtubule-associated proteins that regulate dynamic instability. In addition to regulating microtubule dynamics, RHAMM has been shown to promote cell proliferation through its interaction with ERK1/2. Zhang *et al.*[103] demonstrated that intracellular RHAMM binds to ERK1 and acts as a scaffold protein, forming a complex with ERK2 and MEK1. This complex promotes phosphorylation and dimerization of ERK1/2, which is required for translocation into the nucleus[103,170]. In the human cementifying fibroma cell line, overexpression of RHAMM facilitates phosphorylation and activation of ERK1/2 in nuclei, which promotes the proliferation of the osteoblastic cells[105,171]. In my study, *RHAMM*^{+/+} MDA-MB-231 tumour cells displayed higher levels of nuclear phosphorylated ERK1/2 than *RHAMM*^{-/-} MDA-MB-231 tumour cells in both 2D and 3D cultures, which predicts that RHAMM expression increases cell proliferation of TNBC tumour cells by promoting the activation and translocation of ERK1/2 into the nucleus, where it can phosphorylate substrates important for cell survival and proliferation[172,173]. Collectively, these results

support my hypothesis that RHAMM interacts with ERK1/2 to promote cell proliferation, through the regulation of cell cycle progression and microtubule dynamics.

RHAMM is well characterized for its role in promoting cell motility[109,174–177]. In fact, RHAMM was first identified based on its ability to regulate HRAS-mediated cellular migration[174]. Studies have implicated RHAMM in promoting proliferation in various cell backgrounds, such as in lung cancer[178], smooth muscle[179], and leukemic cells[180]. However, few studies have investigated the role RHAMM specifically plays in promoting breast cancer proliferation and how environmental changes affect the response of RHAMM. In my study, the presence of RHAMM imparted a significantly greater effect on TNBC proliferation/survival in a 3D environment. These results suggest that the proteome regulated by RHAMM depends on the context of the environment, such as whether the cells are in a stiff fibrotic environment as observed in 2D cultures or suspended in cell clusters as observed in 3D cultures. In line with this idea, Veiseh *et al.*[93] demonstrated that suspended 10T½ cells rely on RHAMM as its primary HA receptor, whereas adherent 10T½ cells do not. Therefore, the presence of RHAMM in a 3D environment that suspends tumour cells in a matrix and stimulates cell-to-cell contact has a profound effect on the proliferation/survival of MDA-MB-231 tumour cells, possibly due to differences in the use of RHAMM to bind HA. Further studies using flow cytometry to determine whether there are differences in the levels of RHAMM between MDA-MB-231 tumour cells grown in 2D culture versus 3D culture will provide valuable insight into the mechanism through which RHAMM promotes TNBC proliferation/survival in 3D cultures.

The effect of RHAMM expression on Ki67 expression and ERK1/2 activation in TNBC tumour cells was not different between a 2D and 3D cell culture environment, suggesting

that the effect of RHAMM expression on basic tumour survival phenotypes, such as cell cycle progression and activation of the MAPK pathway, through the activation and translocation of ERK1/2, is independent of a 2D vs. 3D microenvironment. This, along with previous research demonstrating that the MDA-MB-231 tumour cells respond to chemotherapeutic drugs, such as paclitaxel and doxorubicin similarly between 2D and 3D cultures[129], provided the rationale for using 2D cultures to elucidate the effect of RHAMM expression on drug sensitivity in TNBC.

4.2 RHAMM is a biomarker of doxorubicin sensitivity and a therapeutic target for doxorubicin in MDA-MB-231 tumour cells

RHAMM directly interacts with α- and β-tubulins and regulates interphase and mitotic spindle microtubules[126]. Overexpression or inhibition of RHAMM negatively impacts microtubule dynamics[99,126]. Therefore, I hypothesized that knockout of its expression would affect sensitivity or response to paclitaxel, which is a common chemotherapeutic used to treat TNBC that functions by promoting microtubule stability through the assembly and stabilization of tubulin dimers[181]. This increased microtubule stability is detrimental to cells, as it prevents the natural reorganization of microtubules required for interphase and mitotic spindle functioning[181]. In contrast to my hypothesis, RHAMM expression did not confer increased sensitivity to paclitaxel, meaning that both the *RHAMM*^{+/+} and *RHAMM*^{-/-} MDA-MB-231 tumour cells were sensitive to the drug. An *in vitro* study using colon cancer cells demonstrated that paclitaxel promoted a p53-mediated downregulation of RHAMM mRNA expression levels[163]. This raises the possibility that paclitaxel may be promoting the downregulation of RHAMM via p53 such that the *RHAMM*^{+/+} MDA-MB-231 tumour cells display a *RHAMM*^{-/-} phenotype, which would abrogate any differences in sensitivity

based on RHAMM expression. Additional research is required to understand the involvement of p53 and the interplay between microtubule stability by paclitaxel and microtubule instability by RHAMM. Taken together, these results suggest that MDA-MB-231 tumour cells are sensitive to paclitaxel, but RHAMM expression does not increase sensitivity.

Doxorubicin is a commonly used chemotherapy agent for both neoadjuvant and adjuvant chemotherapy in TNBC patients. Doxorubicin promotes apoptosis by intercalating with DNA to prevent DNA synthesis, generating reactive oxygen species that damage DNA, and blocking topoisomerase II to reduce transcription[148,149,182]. Failed efforts to repair the DNA damage induced by doxorubicin ultimately lead to apoptosis. Unfortunately, many TNBC patients develop resistance to doxorubicin, which negatively affects treatment efficacy and reduces their overall survival[183–186]. Despite the development of resistance observed in many patients, a subset of TNBC patients respond well to chemotherapy and have better overall survival rates compared with all breast cancer subtypes[14]. This stresses the importance of discovering biomarkers within the tumour cells and their microenvironments that can indicate susceptibility to treatment. In my study, *RHAMM*^{+/+} MDA-MB-231 tumour cells were more sensitive to doxorubicin than *RHAMM*^{-/-} MDA-MB-231 tumour cells. These results confirm prior work in this lab, showing that *RHAMM*^{-/-} cells are resistant to doxorubicin[166] and underscore the importance of RHAMM expression in promoting doxorubicin sensitivity in TNBC tumour cells. The effect of RHAMM on doxorubicin sensitivity has been explored in other cancer backgrounds such as colon and liver cancer. For example, in colon HCT116 tumour cells and liver HepG2 tumour cells that express p53, doxorubicin treatment reduces the levels of RHAMM mRNA

and promotes cell cycle arrest in G1 and G2[163]. However, limited work has specifically explored the role of RHAMM on doxorubicin sensitivity in breast cancer, including TNBC. My results suggest that RHAMM expression induces sensitivity to doxorubicin in the TNBC MDA-MB-231 cell line possibly due to its ability to promote cell proliferation, which increases the probability of generating doxorubicin-mediated DNA breaks and initiating apoptosis[187–189]. Taken together, these results predict that RHAMM expression provides an indicator of sensitivity to doxorubicin in TNBC and supports my hypothesis that RHAMM expression increases cell sensitivity to therapy.

4.3 Small niches of RHAMM-expressing tumour cells can increase cell proliferation and sensitivity to chemotherapy

RHAMM is commonly found in heterogenous niches throughout tumours, most often at the outer edge and invasive fronts[57,111]. Here, I found that human breast cancer tissue from The Human Protein Atlas denoted as expressing low, medium, and high levels of RHAMM contained an average of approximately 3%, 4% and 29% RHAMM-positive tumour cells, respectively. This is consistent with prior research showing that RHAMM expression can vary between 0 and 50% depending on the levels of tumour differentiation[88,190]. I further showed that only a high *RHAMM*^{+/+} subpopulation increased cell proliferation in co-cultures of *RHAMM*^{+/+} and *RHAMM*^{-/-} MDA-MB-231 tumour cells compared to a completely *RHAMM*^{-/-} monoculture. Further experiments staining the *RHAMM*^{-/-} MDA-MB-231 tumour cells with an anti-GFP antibody will provide insight into the cell type composition of *RHAMM*^{+/+} and *RHAMM*^{-/-} MDA-MB-231 tumour cells at the end of the growth period. These results support a previous study implicating high RHAMM-expressing subsets in promoting breast cancer progression[125]. For example, a 27-gene

RHAMM-dependent signature (RDS), composed of genes associated with the cell cycle, the epithelial-to-mesenchymal pathway, and the mitotic spindle, was identified, where high expression of this gene signature was correlated with lymph node metastasis and a high tumour grade. Furthermore, immunohistochemical and digital spatial transcript profiling demonstrated that RDS gene expression was the highest at the invasive front of tumours, predicting that RDS expression in these focal regions is responsible for activating RHAMM-mediated processes important for invasion and metastasis[125]. The increase in proliferation also raises the possibility that in a heterogeneous environment the $RHAMM^{+/+}$ MDA-MB-231 tumour cells could be undergoing paracrine signalling directly or indirectly that promotes the proliferation of the surrounding $RHAMM^{-/-}$ tumour cells. However, further research is required to understand the specific mechanisms in play. Nevertheless, these results highlight important findings on the ability of small subsets of RHAMM to promote TNBC proliferation.

Using the heterogeneous co-cultures, I also showed that both a low/medium and high $RHAMM^{+/+}$ subpopulation increased the sensitivity of MDA-MB-231 tumour cells to doxorubicin compared to a completely $RHAMM^{-/-}$ environment. Analysis of GFP expression, which was only present in the $RHAMM^{-/-}$ tumour population, demonstrated that the increase in doxorubicin sensitivity was likely attributed to the ability of doxorubicin to specifically target and kill the proliferative $RHAMM^{+/+}$ MDA-MB-231 tumour cells, as the levels of $RHAMM^{-/-}$ MDA-MB-231 tumour cells did not significantly change compared to control as the concentration of doxorubicin increased. To my knowledge, this is the first study to investigate the effect of subsets of tumour cells with varying levels of RHAMM on doxorubicin sensitivity in TNBC.

Taken together, these results suggest that subsets of MDA-MB-231 tumour cells with high RHAMM expression promote tumour proliferation even in an environment of *RHAMM*^{-/-} tumours. Importantly, the ability to specifically target a proliferative and invasive tumour population, such as the *RHAMM*^{+/+} tumour cells, has major clinical implications for TNBC treatment because it can improve drug efficiency and reduce the incidences of off-target apoptosis and toxicity.

4.4 RHAMM increases sensitivity to targeting the MEK/ERK signalling cascade

Western Blot analysis showed that *RHAMM*^{+/+} MDA-MB-231 tumour cells expressed higher levels of phosphorylated ERK1/2 protein than *RHAMM*^{-/-} MDA-MB-231 tumour cells. These results are consistent with studies showing that RHAMM promotes ERK1/2 activation in breast cancer[57,109,191] and that MDA-MB-231 cells express high levels of phosphorylated ERK1/2[192,193]. Many clinical studies have been conducted to investigate the efficacy of various MEK and ERK inhibitors[52]. However, a lack of predictive biomarkers has hindered the successful deployment of these inhibitors in the clinical setting[52]. RHAMM has been shown to interact and form a complex with MEK1/ERK1/2, which affects the subcellular compartmentalization and activation of ERK1/2[103,108,126]. There are numerous therapeutic benefits of targeting the RHAMM/MEK1/ERK1/2 complex because of the conditional expression of RHAMM and limited binding interactions within RHAMM and MEK1. For example, RHAMM expression is upregulated in response to tissue stress, such as those induced by a tumour microenvironment[81]. HA is the ligand of RHAMM, so targeting RHAMM/HA interactions would reduce RHAMM signalling[79,81]. Furthermore, MEK1/2 are the only upstream activators of ERK1/2, so targeting MEK1/2 would inhibit

downstream activation of the MEK/ERK signalling pathway[170,194]. Although the MAPK signalling pathway is important for various basic cellular processes, such as differentiation, motility, and angiogenesis[195], the connection between RHAMM and activation of the MEK/ERK cascade is important for tumorigenesis[105,109,171]. This makes RHAMM expression an indicator of MEK/ERK signalling and a potentially useful biomarker for targeting sensitivity in TNBC. Therefore, I hypothesized that inhibition of the MEK/ERK signalling pathway in *RHAMM*$^{+/+}$ MDA-MB-231 tumour cells by the MEK1/2 inhibitor trametinib would reduce TNBC tumour progression. Leung *et al.*[193] found that MDA-MB-231 cells are the most sensitive to trametinib compared to other breast cancer cell lines, such as MCF-7 and T47D. Consistent with this study and supportive of my hypothesis, *RHAMM*$^{+/+}$ MDA-MB-231 tumour cells were significantly more sensitive to trametinib than *RHAMM*$^{-/-}$ MDA-MB-231 tumour cells. Additionally, the effect of RHAMM expression on drug sensitivity was much stronger in response to trametinib than to doxorubicin. This raises the possibility that trametinib can be used as a novel standard-of-care treatment option for TNBC patients with high RHAMM expression. The possibility of administering trametinib as a standard treatment option has already been demonstrated in ovarian cancer patients. In a phase II/III clinical trial, Gershenson *et al.*[196] found that patients who received trametinib had a higher median progression-free survival than patients who received a standard-of-care treatment drug (i.e., paclitaxel, doxorubicin, topotecan, letrozole or tamoxifen). Furthermore, patients treated with trametinib experienced an overall response rate four times higher than patients treated with the standard-of-care treatment. Future work using *in vivo* models will help to determine whether the effect of RHAMM expression on trametinib sensitivity is translatable to the clinical setting.

Increased sensitivity to MEK1/2 inhibition based on RHAMM expression was further solidified in heterogenous co-cultures of $RHAMM^{+/+}$ and $RHAMM^{-/-}$ MDA-MB-231 tumour cells. Both low/medium and high RHAMM subpopulations increased sensitivity to trametinib compared to a 100% $RHAMM^{-/-}$ environment. This effect was likely due to the selective targeting and killing of the $RHAMM^{+/+}$ tumour cells by trametinib as GFP expression, which was a readout of $RHAMM^{-/-}$ MDA-MB-231 tumour cells, did not significantly change compared to control as the concentration of trametinib increased. The $RHAMM^{+/+}$ MDA-MB-231 monocultures treated with trametinib had a significantly lower IC_{50} than both the low/medium and high co-cultures, possibly due to variations in the number of RHAMM-expressing tumour cells and the level of RHAMM signalling. For instance, while investigating the connection between HA content and RHAMM and CD44 expression, Carvalho et al.[197] found that only 5% of MDA-MB-231 cells were RHAMM-positive. Therefore, the difference in sensitivity to trametinib between the $RHAMM^{+/+}$ MDA-MB-231 monocultures and the low/medium and high co-cultures in my study may result from the co-cultures expressing lower levels of RHAMM in the tumour cells, which could reduce the number of tumour cells that are susceptible to trametinib. Importantly, these results suggest that trametinib sensitivity may be linearly related to the quantity of $RHAMM^{+/+}$ subsets in the tumour microenvironment, which could provide a clinically relevant algorithm to predict trametinib sensitivity. Future experiments using co-cultures of RHAMM-expressing parental MDA-MB-231 tumour cells that do not express GFP with GFP-expressing $RHAMM^{-/-}$ MDA-MB-231 tumour cells to distinguish the two cell types or flow-cytometry to detect RHAMM in the tumour cells via a RHAMM antibody will provide insight on the percentage of RHAMM present in each subpopulation and shed light on whether differences in RHAMM expression affect the magnitude of RHAMM signalling

and sensitivity to trametinib. Together, these results demonstrate that RHAMM expression promotes sensitivity to trametinib in the MDA-MB-231 tumour cells and that the RHAMM signalling pathway could be targeted, specifically through RHAMM/ERK1/2 interactions, to improve drug sensitivity in TNBC.

To identify the mechanisms by which RHAMM induces high trametinib sensitivity, I investigated whether there were changes in ERK1/2 activation in response to trametinib and whether sensitivity was mediated by cell surface RHAMM/HA interactions. In my study, I found that trametinib decreased the protein levels of phosphorylated ERK1/2 in the *RHAMM*^{+/+} MDA-MB-231 tumour cells. This is consistent with multiple studies showing that trametinib decreases phosphorylated ERK1/2 expression *in vitro*[193,198,199]. Additional experiments exploring the effect of trametinib on phosphorylated ERK1/2 expression in the *RHAMM*^{-/-} MDA-MB-231 tumour cells are required to understand whether the mechanism of inhibition is facilitated by blocking the activity of ERK1/2 or by modifying subcellular localization.

RHAMM plays a central role in mediating changes in HA content in the microenvironment[197], and interactions between HA, and the HA receptors, CD44 and RHAMM, promote activation of ERK1/2[108], including in MDA-MB-231 tumour cells[109]. Here, I determined that trametinib sensitivity may be mediated by cell surface RHAMM/HA interactions. In my study, blocking cell surface RHAMM/HA interaction with a cyclized peptide that mimics the HA binding region of RHAMM rescued the viability of *RHAMM*^{+/+} MDA-MB-231 tumour cells treated with a low concentration of trametinib, suggesting that interactions between cell surface RHAMM and HA are required to facilitate trametinib-mediated apoptosis. Future experiments examining ERK1/2

activation in peptide-treated MDA-MB-231 tumour cells should be conducted to determine whether blockage of cell surface RHAMM/HA interactions affects ERK1/2 expression.

A biomarker, such as RHAMM, that can identify treatment-sensitive tumours is an asset in overcoming chemoresistance and dose-limiting toxicities, which are primary limitations to the success of clinical TNBC treatments[200]. Taken together, these results support the hypothesis that RHAMM expression increases sensitivity to therapy, specifically with trametinib, and highlight novel avenues through which RHAMM expression can be used for targeted treatment against TNBC.

4.5 RHAMM promotes synergy between paclitaxel and trametinib in a schedule- and concentration-dependent manner

Monotherapies aimed at targeting specific hyper-activated pathways or mutated genes have shown better responses in clinical trials compared to generalized treatment[201,202]. However, tumours are well characterized for their genomic instabilities, and these instabilities often lead to genetic alterations that provide novel resistance to treatments that were once effective[203]. Combination therapies that target multiple genes simultaneously help to overcome this limitation, as they prevent aberrant pathways from working in tandem to increase resistance. Determining the most effective drug combinations is a challenge due to the vast number of combinations possible. Additionally, effectiveness can also depend on the schedule and concentrations at which the drugs are administered[204]. For instance, Vogus *et al.*[205] found that sequentially exposing MDA-MB-231 cells to gemcitabine followed by doxorubicin inhibited more cell growth than exposure to doxorubicin followed

by gemcitabine or simultaneous exposure and significantly increased caspase activity compared to single-agent exposure to doxorubicin.

To understand the mechanisms that mediate doxorubicin resistance in breast cancer, Christowitz *et al.*[206] explored the involvement of signalling pathways, such as the MAPK/ERK and PI3K/Akt pathways, as they have been shown to protect cells from apoptosis through the regulation of cell proliferation, metabolism and gene transcription[207–209]. Between the MAPK/ERK and PI3K/Akt pathways, doxorubicin resistance in breast tumours was found to be associated with increases in phosphorylated ERK1/2 expression, whereas there were no significant changes in the expression of PI3K/Akt markers[206]; thus providing the rationale for inhibiting the MAPK/ERK pathway to improve doxorubicin efficacy. In this study, the combination of doxorubicin and trametinib was hypothesized to synergistically promote apoptosis of the *RHAMM*^{+/+} MDA-MB-231 tumour cells, since RHAMM has been implicated in promoting the proliferation of these tumour cells, likely through its interaction with the MEK/ERK cascade. Furthermore, RHAMM expression increased the sensitivity of the *RHAMM*^{+/+} MDA-MB-231 tumour cells to both doxorubicin and trametinib. Surprisingly, the combination of doxorubicin and trametinib either simultaneously or sequentially in the *RHAMM*^{+/+} MDA-MB-231 tumour cells did not provide synergistic effects. Prior research has shown that trametinib can antagonize the P-glycoprotein-mediated efflux of doxorubicin to increase the anti-tumour effect of doxorubicin[210,211]. In my study, the concentration of doxorubicin administered was between 20 to 40 times higher than trametinib because the MDA-MB-231 cells were more resistant to doxorubicin. Thus, at the concentrations tested, there may not have been enough trametinib present to prevent P-glycoprotein, for example, from binding to and expelling

doxorubicin from the cells. Further research investigating the synergistic effect of doxorubicin at much lower concentrations can address this theory.

Apart from its role in proliferation, RHAMM is known to interact with microtubules and regulate their dynamics. RHAMM co-localizes with the mitotic spindles of dividing cells and along the entire length of microtubules in interphase cells[98–100]. Although RHAMM expression did not increase paclitaxel sensitivity, the MDA-MB-231 tumour cells were still sensitive to paclitaxel. Since both paclitaxel and RHAMM have strong connections to microtubules, I hypothesized that paclitaxel may enhance the RHAMM-dependent effect of trametinib. In my study, the sequential administration of paclitaxel followed by trametinib was synergistic in the $RHAMM^{+/+}$ MDA-MB-231 tumour cells, meaning that the drugs worked together to promote cell death more than either drug alone. Multiple preclinical and clinical studies have shown that the combination of paclitaxel and trametinib is a promising combination treatment. For example, a pilot study found that daily administration of paclitaxel and trametinib resulted in either a partial response or a stable disease in eight out of twelve anaplastic thyroid cancer patients, with only two patients discontinuing treatment due to toxicity[212]. In a preclinical model of pancreatic ductal adenocarcinoma, the combination of trametinib with paclitaxel had a trend towards an additive effect on tumour reduction and significantly increased the median survival compared to the control[213]. In this study, the time of administration and the concentrations used were major determinants of synergy. I hypothesized that the addition of paclitaxel before trametinib allows paclitaxel to induce mitotic arrest and prevent RHAMM from promoting cell cycle progression, making it easier for trametinib to induce apoptosis through its inhibition of the MEK/ERK cascade. In line with this idea, I hypothesized that

since *RHAMM*^{+/+} MDA-MB-231 tumour cells are highly sensitive to trametinib, the addition of trametinib before paclitaxel prevents paclitaxel from imparting any synergistic effect because most of the cells are likely already dead. An analysis of the cell cycle distribution of lung cancer cells after treatment with paclitaxel found that paclitaxel can induce p53-dependent G1-like arrest after multiple cell cycles, so long as the concentration of paclitaxel is low[214]. Trametinib has been shown to arrest cells in the G1 phase[215–217]. Thus, in this study, the addition of a low concentration of paclitaxel could have arrested the MDA-MB-231 tumour cells in G1, providing an ideal environment for trametinib. Additional research exploring the cell cycle distribution of the MDA-MB-231 tumour cells after combination treatment with paclitaxel and trametinib will provide a further understanding of how these drugs work in tandem to induce apoptosis. The tumour environment is a complex system that relies on interactions between multiple cell pathways to evade apoptosis and survive. Taken together, my results suggest that targeting the pathways and interactions responsible for RHAMM-mediated proliferation and survival, through paclitaxel and trametinib, can prove beneficial for TNBC treatment.

4.6   Limitations and Future Directions

This study provided insight into the importance of RHAMM on drug sensitivity in TNBC. While these results were beneficial in expanding our understanding of RHAMM function, additional research is required to elucidate the specific mechanisms that promote RHAMM-mediated proliferation and drug sensitivity. For example, differentially staining the *RHAMM*^{+/+} and *RHAMM*^{-/-} MDA-MB-231 tumour cells in the heterogenous co-cultures will allow us to determine whether the *RHAMM*^{+/+} cells are promoting proliferation of the surrounding *RHAMM*^{-/-} cells through paracrine signalling or whether the *RHAMM*^{+/+} cells

are proliferating so rapidly they form a larger niche than originally observed. Immunofluorescence staining and western blot assays of Ki67 and Cleaved Caspase-3 will provide further confirmation of cell death upon doxorubicin and trametinib treatment in $RHAMM^{+/+}$ breast cancer cells. Both RHAMM and the drugs administered in this study have been shown to affect cell cycle progression. For example, RHAMM silencing has been shown to impact mitotic progression[164]. MDA-MB-231 tumour cells treated with trametinib and doxorubicin are arrested in the G1[215,216] and G2/M[205,218] phases of the cell cycle, respectively. Thus, cell cycle analyses will help determine the cell cycle distribution of cells upon loss of RHAMM expression or drug administration. Knowing where TNBC cells are in the cell cycle may inform which cell cycle proteins are upregulated or downregulated. This knowledge may lead to developments in targeted combination therapy that can promote and/or take advantage of arrested cells.

One of the limitations of this study was that all the experiments were conducted using the invasive MDA-MB-231 TNBC cell line. Breast cancer cell lines vary in their level of invasiveness and tumorigenicity. This can affect which signalling pathways are utilized and how the cells respond to stimuli. For instance, Hamilton *et al.*[109] found that the more invasive MDA-MB-231 cell line expressed higher levels of HA, CD44, RHAMM, and ERK1/2 than the less invasive MCF7 cell line. Furthermore, co-localization of RHAMM, CD44 and ERK1/2 only occurred in the MDA-MB-231 cell line, and this interaction is important for the motile capabilities of the cells. Thus, future studies exploring the effect of RHAMM expression on proliferation and drug sensitivity in other TNCB cell lines or less invasive cell lines, such as the MCF7 cell line, will aid in determining whether the effect of RHAMM is linked to the invasiveness of the breast cancer cells.

Using 2D cultures in this study allowed for the initial determination of the effect of RHAMM expression on drug sensitivity in the TNBC tumour cells. However, the response of tumour cells to various stimuli depends on the context of their environment. For example, Vogus *et al.*[205] found that treating MDA-MB-231 cells with gemcitabine followed by doxorubicin *in vitro* was the most synergistic administration schedule. However, *in vivo*, the order in which the drugs were administered made no difference in tumour inhibition[205]. Using patient-derived tumours, Cromwell *et al.*[219] found that the IC_{50} for paclitaxel was ~100 times higher than the IC_{50}s for trametinib and romidepsin and higher than the recorded IC_{50}s for paclitaxel in 2D culture. Future studies using 3D cultures and *in vivo* mouse models will address the limitations of 2D cultures. This will be important in determining whether the effect of RHAMM expression on drug sensitivity is translatable to the human environment.

4.7   Significance and Conclusions

The novel findings presented in this study suggest that RHAMM is a biomarker and therapeutic target in TNBC. RHAMM promotes the proliferation and survival of TNBC tumour cells and induces sensitivity to the conventional breast cancer chemotherapy drug doxorubicin and a novel targeted breast cancer therapy drug trametinib. In breast cancer, RHAMM is observed in heterogeneous niches at the peripheral edge of tumours[125]. The interaction of RHAMM and HA within these niches activates RHAMM signalling that promotes invasive growth and metastasis[125]. Importantly, this study suggests that these proliferative and invasive *RHAMM*$^{+/+}$ niches can be targeted for apoptosis by doxorubicin and trametinib, which has vast implications for the clinical treatment of TNBC. Furthermore, this study suggests that various facets of the RHAMM signalling pathway,

such as its interaction with microtubules and the MEK/ERK cascade, can be targeted through combination therapy to promote increased drug sensitivity and apoptosis.

Developing effective targeted treatments for TNBC is important as most TNBC patients develop resistance to standard-of-care chemotherapy treatments and, as such, experience poor overall survival outcomes. TNBC is a highly heterogeneous and complex disease. Biomarkers that aid in identifying proliferative tumour populations can inform on the underlying biology of the tumour, which helps immensely in promoting successful treatment response and providing a personalized cancer treatment strategy.

References

1.   Lee, S. Breast cancer statistics. *Canadian Cancer Society* https://cancer.ca/en/cancer-information/cancer-types/breast/statistics.

2.   Brenner, D. R. *et al.* Projected estimates of cancer in Canada in 2022. *CMAJ* **194**, E601–E607 (2022).

3.   Malhotra, G. K., Zhao, X., Band, H. & Band, V. Histological, molecular and functional subtypes of breast cancers. *Cancer Biol Ther* **10**, 955–960 (2010).

4.   Akram, M., Iqbal, M., Daniyal, M. & Khan, A. U. Awareness and current knowledge of breast cancer. *Biol Res* **50**, 33 (2017).

5.   Sørlie, T. *et al.* Gene expression patterns of breast carcinomas distinguish tumor subclasses with clinical implications. *Proc Natl Acad Sci U S A* **98**, 10869–10874 (2001).

6.   Weigelt, B., Baehner, F. L. & Reis-Filho, J. S. The contribution of gene expression profiling to breast cancer classification, prognostication and prediction: a retrospective of the last decade. *The Journal of Pathology* **220**, 263–280 (2010).

7.   Foulkes, W. D., Smith, I. E. & Reis-Filho, J. S. Triple-negative breast cancer. *N Engl J Med* **363**, 1938–1948 (2010).

8.   Aysola, K. *et al.* Triple Negative Breast Cancer - An Overview. *Hereditary Genet* **2013**, 001 (2013).

9.   Collignon, J., Lousberg, L., Schroeder, H. & Jerusalem, G. Triple-negative breast cancer: treatment challenges and solutions. *Breast Cancer (Dove Med Press)* **8**, 93–107 (2016).

10.   Heitz, F. *et al.* Triple-negative and HER2-overexpressing breast cancers exhibit an elevated risk and an earlier occurrence of cerebral metastases. *Eur J Cancer* **45**, 2792–2798 (2009).

11.   Perou, C. M. *et al.* Molecular portraits of human breast tumours. *Nature* **406**, 747–752 (2000).

12.   Yin, L., Duan, J.-J., Bian, X.-W. & Yu, S. Triple-negative breast cancer molecular subtyping and treatment progress. *Breast Cancer Research* **22**, 61 (2020).

13.   Lehmann, B. D. *et al.* Identification of human triple-negative breast cancer subtypes and preclinical models for selection of targeted therapies. *J Clin Invest* **121**, 2750–2767 (2011).

14.   Liedtke, C. *et al.* Response to neoadjuvant therapy and long-term survival in patients with triple-negative breast cancer. *J Clin Oncol* **26**, 1275–1281 (2008).

15.   Lin, N. U. *et al.* Clinicopathologic features, patterns of recurrence, and survival among women with triple-negative breast cancer in the National Comprehensive Cancer Network. *Cancer* **118**, 5463–5472 (2012).

16.   Li, X. *et al.* Triple-negative breast cancer has worse overall survival and cause-specific survival than non-triple-negative breast cancer. *Breast Cancer Res Treat* **161**, 279–287 (2017).

17.   Dent, R. *et al.* Triple-negative breast cancer: clinical features and patterns of recurrence. *Clin Cancer Res* **13**, 4429–4434 (2007).

18.   Penault-Llorca, F. & Viale, G. Pathological and molecular diagnosis of triple-negative breast cancer: a clinical perspective. *Ann Oncol* **23 Suppl 6**, vi19-22 (2012).

19.   Goossens, N., Nakagawa, S., Sun, X. & Hoshida, Y. Cancer biomarker discovery and validation. *Transl Cancer Res* **4**, 256–269 (2015).

20.   Carey, L. A. *et al.* The triple negative paradox: primary tumor chemosensitivity of breast cancer subtypes. *Clin Cancer Res* **13**, 2329–2334 (2007).

21.   Masuda, H. *et al.* Differential response to neoadjuvant chemotherapy among 7 triple-negative breast cancer molecular subtypes. *Clin Cancer Res* **19**, 5533–5540 (2013).

22.   Lehmann, B. D. & Pietenpol, J. A. Identification and use of biomarkers in treatment strategies for triple-negative breast cancer subtypes. *J Pathol* **232**, 142–150 (2014).

23.   Hoeijmakers, J. H. Genome maintenance mechanisms for preventing cancer. *Nature* **411**, 366–374 (2001).

24.   Chatterjee, N. & Walker, G. C. Mechanisms of DNA damage, repair and mutagenesis. *Environ Mol Mutagen* **58**, 235–263 (2017).

25.   Couch, F. J. *et al.* Inherited mutations in 17 breast cancer susceptibility genes among a large triple-negative breast cancer cohort unselected for family history of breast cancer. *J Clin Oncol* **33**, 304–311 (2015).

26.   Bianchini, G., De Angelis, C., Licata, L. & Gianni, L. Treatment landscape of triple-negative breast cancer — expanded options, evolving needs. *Nat Rev Clin Oncol* **19**, 91–113 (2022).

27.   Robson, M. *et al.* Olaparib for Metastatic Breast Cancer in Patients with a Germline BRCA Mutation. *New England Journal of Medicine* **377**, 523–533 (2017).

28.   Litton, J. K. *et al.* Talazoparib in Patients with Advanced Breast Cancer and a Germline BRCA Mutation. *New England Journal of Medicine* **379**, 753–763 (2018).

29.   Diéras, V. *et al.* Veliparib with carboplatin and paclitaxel in BRCA-mutated advanced breast cancer (BROCADE3): a randomised, double-blind, placebo-controlled, phase 3 trial. *Lancet Oncol* **21**, 1269–1282 (2020).

30. Litton, J. K. *et al.* Neoadjuvant Talazoparib for Patients With Operable Breast Cancer With a Germline BRCA Pathogenic Variant. *J Clin Oncol* **38**, 388–394 (2020).

31. Tutt, A. N. J. *et al.* Adjuvant Olaparib for Patients with BRCA1- or BRCA2-Mutated Breast Cancer. *New England Journal of Medicine* **384**, 2394–2405 (2021).

32. Traina, T. A. *et al.* Enzalutamide for the Treatment of Androgen Receptor-Expressing Triple-Negative Breast Cancer. *J Clin Oncol* **36**, 884–890 (2018).

33. Gucalp, A. *et al.* Phase II trial of bicalutamide in patients with androgen receptor-positive, estrogen receptor-negative metastatic Breast Cancer. *Clin Cancer Res* **19**, 5505–5512 (2013).

34. Bareche, Y. *et al.* Unravelling triple-negative breast cancer molecular heterogeneity using an integrative multiomic analysis. *Ann Oncol* **29**, 895–902 (2018).

35. Lehmann, B. D. *et al.* TBCRC 032 IB/II Multicenter Study: Molecular Insights to AR Antagonist and PI3K Inhibitor Efficacy in Patients with AR+ Metastatic Triple-Negative Breast Cancer. *Clin Cancer Res* **26**, 2111–2123 (2020).

36. Cleator, S., Heller, W. & Coombes, R. C. Triple-negative breast cancer: therapeutic options. *Lancet Oncol* **8**, 235–244 (2007).

37. Nielsen, T. O. *et al.* Immunohistochemical and clinical characterization of the basal-like subtype of invasive breast carcinoma. *Clin Cancer Res* **10**, 5367–5374 (2004).

38. Livasy, C. A. *et al.* Phenotypic evaluation of the basal-like subtype of invasive breast carcinoma. *Mod Pathol* **19**, 264–271 (2006).

39. Carey, L. A. *et al.* TBCRC 001: randomized phase II study of cetuximab in combination with carboplatin in stage IV triple-negative breast cancer. *J Clin Oncol* **30**, 2615–2623 (2012).

40. Baselga, J. *et al.* Randomized Phase II Study of the Anti–Epidermal Growth Factor Receptor Monoclonal Antibody Cetuximab With Cisplatin Versus Cisplatin Alone in Patients With Metastatic Triple-Negative Breast Cancer. *J Clin Oncol* **31**, 2586–2592 (2013).

41. Nanda, R. *et al.* Pembrolizumab in Patients With Advanced Triple-Negative Breast Cancer: Phase Ib KEYNOTE-012 Study. *J Clin Oncol* **34**, 2460–2467 (2016).

42. Emens, L. A. *et al.* Long-term Clinical Outcomes and Biomarker Analyses of Atezolizumab Therapy for Patients With Metastatic Triple-Negative Breast Cancer: A Phase 1 Study. *JAMA Oncol* **5**, 74–82 (2019).

43. Voorwerk, L. *et al.* Immune induction strategies in metastatic triple-negative breast cancer to enhance the sensitivity to PD-1 blockade: the TONIC trial. *Nat Med* **25**, 920–928 (2019).

44.   Gibson, G. R., Qian, D., Ku, J. K. & Lai, L. L. Metaplastic breast cancer: clinical features and outcomes. *Am Surg* **71**, 725–730 (2005).

45.   Maqbool, M., Bekele, F. & Fekadu, G. Treatment Strategies Against Triple-Negative Breast Cancer: An Updated Review. *Breast Cancer (Dove Med Press)* **14**, 15–24 (2022).

46.   Basho, R. K. *et al.* Targeting the PI3K/AKT/mTOR Pathway for the Treatment of Mesenchymal Triple-Negative Breast Cancer: Evidence From a Phase 1 Trial of mTOR Inhibition in Combination With Liposomal Doxorubicin and Bevacizumab. *JAMA Oncology* **3**, 509–515 (2017).

47.   Qiu, M. *et al.* Specific inhibition of Notch1 signaling enhances the antitumor efficacy of chemotherapy in triple negative breast cancer through reduction of cancer stem cells. *Cancer Lett* **328**, 261–270 (2013).

48.   Izrailit, J. & Reedijk, M. Developmental pathways in breast cancer and breast tumor-initiating cells: Therapeutic implications. *Cancer Letters* **317**, 115–126 (2012).

49.   Locatelli, M. A. *et al.* Phase I study of the gamma secretase inhibitor PF-03084014 in combination with docetaxel in patients with advanced triple-negative breast cancer. *Oncotarget* **8**, 2320–2328 (2016).

50.   Robinson, M. J. & Cobb, M. H. Mitogen-activated protein kinase pathways. *Curr Opin Cell Biol* **9**, 180–186 (1997).

51.   Chang, L. & Karin, M. Mammalian MAP kinase signalling cascades. *Nature* **410**, 37–40 (2001).

52.   Zhao, Y. & Adjei, A. A. The clinical development of MEK inhibitors. *Nat Rev Clin Oncol* **11**, 385–400 (2014).

53.   Johnson, G. L. & Vaillancourt, R. R. Sequential protein kinase reactions controlling cell growth and differentiation. *Curr Opin Cell Biol* **6**, 230–238 (1994).

54.   Meloche, S. & Pouysségur, J. The ERK1/2 mitogen-activated protein kinase pathway as a master regulator of the G1- to S-phase transition. *Oncogene* **26**, 3227–3239 (2007).

55.   Shaul, Y. D. & Seger, R. The MEK/ERK cascade: from signaling specificity to diverse functions. *Biochim Biophys Acta* **1773**, 1213–1226 (2007).

56.   Adeyinka, A. *et al.* Activated mitogen-activated protein kinase expression during human breast tumorigenesis and breast cancer progression. *Clin Cancer Res* **8**, 1747–1753 (2002).

57.   Wang, C. *et al.* The overexpression of RHAMM, a hyaluronan-binding protein that regulates ras signaling, correlates with overexpression of mitogen-activated protein kinase

and is a significant parameter in breast cancer progression. *Clin Cancer Res* **4**, 567–576 (1998).

58.   Gagliardi, M. *et al.* Differential functions of ERK1 and ERK2 in lung metastasis processes in triple-negative breast cancer. *Sci Rep* **10**, 8537 (2020).

59.   Bartholomeusz, C. *et al.* High ERK Protein Expression Levels Correlate with Shorter Survival in Triple-Negative Breast Cancer Patients. *Oncologist* **17**, 766–774 (2012).

60.   Jiang, W., Wang, X., Zhang, C., Xue, L. & Yang, L. Expression and clinical significance of MAPK and EGFR in triple-negative breast cancer. *Oncol Lett* **19**, 1842–1848 (2020).

61.   Na, J., Furue, M. K. & Andrews, P. W. Inhibition of ERK1/2 prevents neural and mesendodermal differentiation and promotes human embryonic stem cell self-renewal. *Stem Cell Res* **5**, 157–169 (2010).

62.   D'Angelo, G., Struman, I., Martial, J. & Weiner, R. I. Activation of mitogen-activated protein kinases by vascular endothelial growth factor and basic fibroblast growth factor in capillary endothelial cells is inhibited by the antiangiogenic factor 16-kDa N-terminal fragment of prolactin. *Proc Natl Acad Sci U S A* **92**, 6374–6378 (1995).

63.   Wu, P.-K. & Park, J.-I. MEK1/2 Inhibitors: Molecular Activity and Resistance Mechanisms. *Semin Oncol* **42**, 849–862 (2015).

64.   Flaherty, K. T. *et al.* Combined BRAF and MEK Inhibition in Melanoma with BRAF V600 Mutations. *New England Journal of Medicine* **367**, 1694–1703 (2012).

65.   Infante, J. R. *et al.* Safety, pharmacokinetic, pharmacodynamic, and efficacy data for the oral MEK inhibitor trametinib: a phase 1 dose-escalation trial. *Lancet Oncol* **13**, 773–781 (2012).

66.   Mekinist (trametinib) tablets, 0.5 mg, 1 mg, 2 mg. 8.

67.   Novartis Pharmaceuticals. *A Phase Ib, Open-label, Multi-center, Dose-escalation Study of Oral BKM120 in Combination With Oral GSK1120212 in Adult Patients With Selected Advanced Solid Tumors.* https://clinicaltrials.gov/ct2/show/NCT01155453 (2020).

68.   National Cancer Institute (NCI). *An Open Label, Two-Part, Phase Ib/II Study to Investigate the Safety, Pharmacokinetics, Pharmacodynamics, and Clinical Activity of the MEK Inhibitor Trametinib and the BCL2-Family Inhibitor Navitoclax (ABT-263) in Combination in Subjects With KRAS or NRAS Mutation-Positive Advanced Solid Tumors.* https://clinicaltrials.gov/ct2/show/NCT02079740 (2022).

69.   Kurzrock, R. *et al.* Phase I dose-escalation of the oral MEK1/2 inhibitor GSK1120212 (GSK212) dosed in combination with the oral AKT inhibitor GSK2141795 (GSK795). *JCO* **29**, 3085–3085 (2011).

70.   Ramaswamy, B. *et al.* Abstract LB-216: NCI 9455: Phase II study of trametinib followed by trametinib plus AKT inhibitor,GSK2141795 in patients with advanced triple negative breast cancer. *Cancer Research* **76**, LB-216 (2016).

71.   LoRusso, P. M. *et al.* Phase I pharmacokinetic and pharmacodynamic study of the oral MAPK/ERK kinase inhibitor PD-0325901 in patients with advanced cancers. *Clin Cancer Res* **16**, 1924–1937 (2010).

72.   Boasberg, P. D. *et al.* Pilot study of PD-0325901 in previously treated patients with advanced melanoma, breast cancer, and colon cancer. *Cancer Chemother Pharmacol* **68**, 547–552 (2011).

73.   Mita, M. M. *et al.* A phase Ia study of CC-90003, a selective extracellular signal-regulated kinase (ERK) inhibitor, in patients with relapsed or refractory BRAF or RAS-mutant tumors. *JCO* **35**, 2577–2577 (2017).

74.   Al-Mahayri, Z. N., Patrinos, G. P. & Ali, B. R. Toxicity and Pharmacogenomic Biomarkers in Breast Cancer Chemotherapy. *Front Pharmacol* **11**, 445 (2020).

75.   Ree, A. H., Meltzer, S., Flatmark, K., Dueland, S. & Kalanxhi, E. Biomarkers of Treatment Toxicity in Combined-Modality Cancer Therapies with Radiation and Systemic Drugs: Study Design, Multiplex Methods, Molecular Networks. *Int J Mol Sci* **15**, 22835–22856 (2014).

76.   BioRender. https://biorender.com/.

77.   Arvelo, F., Sojo, F. & Cotte, C. Tumour progression and metastasis. *Ecancermedicalscience* **10**, 617 (2016).

78.   Maxwell, C. A., McCarthy, J. & Turley, E. Cell-surface and mitotic-spindle RHAMM: moonlighting or dual oncogenic functions? *Journal of Cell Science* **121**, 925–932 (2008).

79.   Misra, S., Hascall, V. C., Markwald, R. R. & Ghatak, S. Interactions between Hyaluronan and Its Receptors (CD44, RHAMM) Regulate the Activities of Inflammation and Cancer. *Front Immunol* **6**, 201 (2015).

80.   Tavianatou, A. G. *et al.* Hyaluronan: molecular size-dependent signaling and biological functions in inflammation and cancer. *The FEBS Journal* **286**, 2883–2908 (2019).

81.   Tolg, C., McCarthy, J. B., Yazdani, A. & Turley, E. A. Hyaluronan and RHAMM in Wound Repair and the "Cancerization" of Stromal Tissues. *Biomed Res Int* **2014**, 103923 (2014).

82.   Monzon, M. E. *et al.* Reactive oxygen species and hyaluronidase 2 regulate airway epithelial hyaluronan fragmentation. *J Biol Chem* **285**, 26126–26134 (2010).

83.   Garantziotis, S. & Savani, R. C. Hyaluronan biology: A complex balancing act of structure, function, location and context. *Matrix Biol* **78–79**, 1–10 (2019).

84.   Liu, M., Tolg, C. & Turley, E. Dissecting the Dual Nature of Hyaluronan in the Tumor Microenvironment. *Front Immunol* **10**, 947 (2019).

85.   Velesiotis, C., Vasileiou, S. & Vynios, D. H. A guide to hyaluronan and related enzymes in breast cancer: biological significance and diagnostic value. *FEBS J* **286**, 3057–3074 (2019).

86.   Heldin, P. *et al.* Deregulation of hyaluronan synthesis, degradation and binding promotes breast cancer. *J Biochem* **154**, 395–408 (2013).

87.   Greiner, J. *et al.* Receptor for hyaluronan acid-mediated motility (RHAMM) is a new immunogenic leukemia-associated antigen in acute and chronic myeloid leukemia. *Exp Hematol* **30**, 1029–1035 (2002).

88.   Chen, Y.-T., Chen, Z. & Du, Y.-C. N. Immunohistochemical analysis of RHAMM expression in normal and neoplastic human tissues: a cell cycle protein with distinctive expression in mitotic cells and testicular germ cells. *Oncotarget* **9**, 20941–20952 (2018).

89.   Wu, M. *et al.* A novel role of low molecular weight hyaluronan in breast cancer metastasis. *FASEB J* **29**, 1290–1298 (2015).

90.   Kornovski, B. S., McCoshen, J., Kredentser, J. & Turley, E. The regulation of sperm motility by a novel hyaluronan receptor. *Fertil Steril* **61**, 935–940 (1994).

91.   Fieber, C. *et al.* Characterisation of the murine gene encoding the intracellular hyaluronan receptor IHABP (RHAMM). *Gene* **226**, 41–50 (1999).

92.   Line, A. *et al.* Characterisation of tumour-associated antigens in colon cancer. *Cancer Immunol Immunother* **51**, 574–582 (2002).

93.   Veiseh, M. *et al.* Cellular heterogeneity profiling by hyaluronan probes reveals an invasive but slow-growing breast tumor subset. *Proceedings of the National Academy of Sciences* **111**, E1731–E1739 (2014).

94.   Symonette, C. J. *et al.* Hyaluronan-Phosphatidylethanolamine Polymers Form Pericellular Coats on Keratinocytes and Promote Basal Keratinocyte Proliferation. *BioMed Research International* **2014**, e727459 (2014).

95.   Cho, R. J. *et al.* Transcriptional regulation and function during the human cell cycle. *Nat Genet* **27**, 48–54 (2001).

96.   Whitfield, M. L. *et al.* Identification of Genes Periodically Expressed in the Human Cell Cycle and Their Expression in Tumors. *MBoC* **13**, 1977–2000 (2002).

97.   Yang, C.-W. *et al.* Integrative genomics based identification of potential human hepatocarcinogenesis-associated cell cycle regulators: RHAMM as an example. *Biochem Biophys Res Commun* **330**, 489–497 (2005).

98.   Maxwell, C. A. *et al.* RHAMM is a centrosomal protein that interacts with dynein and maintains spindle pole stability. *Mol Biol Cell* **14**, 2262–2276 (2003).

99.   Maxwell, C. A., Keats, J. J., Belch, A. R., Pilarski, L. M. & Reiman, T. Receptor for hyaluronan-mediated motility correlates with centrosome abnormalities in multiple myeloma and maintains mitotic integrity. *Cancer Res* **65**, 850–860 (2005).

100.   Assmann, V., Jenkinson, D., Marshall, J. F. & Hart, I. R. The intracellular hyaluronan receptor RHAMM/IHABP interacts with microtubules and actin filaments. *J Cell Sci* **112 (Pt 22)**, 3943–3954 (1999).

101.   Groen, A. C. *et al.* XRHAMM functions in ran-dependent microtubule nucleation and pole formation during anastral spindle assembly. *Curr Biol* **14**, 1801–1811 (2004).

102.   Turley, E. A., Noble, P. W. & Bourguignon, L. Y. W. Signaling properties of hyaluronan receptors. *J Biol Chem* **277**, 4589–4592 (2002).

103.   Zhang, S. *et al.* The hyaluronan receptor RHAMM regulates extracellular-regulated kinase. *J Biol Chem* **273**, 11342–11348 (1998).

104.   Du, Y.-C. N., Chou, C.-K., Klimstra, D. S. & Varmus, H. Receptor for hyaluronan-mediated motility isoform B promotes liver metastasis in a mouse model of multistep tumorigenesis and a tail vein assay for metastasis. *Proc Natl Acad Sci U S A* **108**, 16753–16758 (2011).

105.   Hatano, H. *et al.* RHAMM/ERK interaction induces proliferative activities of cementifying fibroma cells through a mechanism based on the CD44–EGFR. *Lab Invest* **91**, 379–391 (2011).

106.   Samuel, S. K. *et al.* TGF-beta 1 stimulation of cell locomotion utilizes the hyaluronan receptor RHAMM and hyaluronan. *J Cell Biol* **123**, 749–758 (1993).

107.   Park, D. *et al.* Hyaluronic Acid Promotes Angiogenesis by Inducing RHAMM-TGFβ Receptor Interaction via CD44-PKCδ. *Mol Cells* **33**, 563–574 (2012).

108.   Tolg, C. *et al.* Rhamm-/- fibroblasts are defective in CD44-mediated ERK1,2 motogenic signaling, leading to defective skin wound repair. *J Cell Biol* **175**, 1017–1028 (2006).

109.   Hamilton, S. R. *et al.* The hyaluronan receptors CD44 and Rhamm (CD168) form complexes with ERK1,2 that sustain high basal motility in breast cancer cells. *J Biol Chem* **282**, 16667–16680 (2007).

110.   Caon, I. *et al.* Revisiting the hallmarks of cancer: The role of hyaluronan. *Semin Cancer Biol* **62**, 9–19 (2020).

111.   Assmann, V. *et al.* The pattern of expression of the microtubule-binding protein RHAMM/IHABP in mammary carcinoma suggests a role in the invasive behaviour of tumour cells. *J Pathol* **195**, 191–196 (2001).

112. Bièche, I., Tozlu, S., Girault, I. & Lidereau, R. Identification of a three-gene expression signature of poor-prognosis breast carcinoma. *Molecular Cancer* **3**, 37 (2004).

113. Schütze, A. *et al.* RHAMM splice variants confer radiosensitivity in human breast cancer cell lines. *Oncotarget* **7**, 21428–21440 (2016).

114. Kahl, I. *et al.* The cell cycle-related genes RHAMM, AURKA, TPX2, PLK1, and PLK4 are associated with the poor prognosis of breast cancer patients. *Journal of Cellular Biochemistry* **123**, 581–600 (2022).

115. Turley, E. A., Belch, A. J., Poppema, S. & Pilarski, L. M. Expression and function of a receptor for hyaluronan-mediated motility on normal and malignant B lymphocytes. *Blood* **81**, 446–453 (1993).

116. Maxwell, C. A. *et al.* RHAMM expression and isoform balance predict aggressive disease and poor survival in multiple myeloma. *Blood* **104**, 1151–1158 (2004).

117. Zhu, S.-W. *et al.* Overexpression of CD168 is related to poor prognosis in oral squamous cell carcinoma. *Oral Dis* **28**, 364–372 (2022).

118. Rizzardi, A. E. *et al.* Elevated HA and HMMR are associated with biochemical failure in patients with intermediate grade prostate tumors. *Cancer* **120**, 1800–1809 (2014).

119. Zlobec, I., Baker, K., Terracciano, L. M. & Lugli, A. RHAMM, p21 combined phenotype identifies microsatellite instability-high colorectal cancers with a highly adverse prognosis. *Clin Cancer Res* **14**, 3798–3806 (2008).

120. Zlobec, I. *et al.* Role of RHAMM within the hierarchy of well-established prognostic factors in colorectal cancer. *Gut* **57**, 1413–1419 (2008).

121. Lugli, A. *et al.* Overexpression of the receptor for hyaluronic acid mediated motility is an independent adverse prognostic factor in colorectal cancer. *Mod Pathol* **19**, 1302–1309 (2006).

122. Ishigami, S. *et al.* Prognostic impact of CD168 expression in gastric cancer. *BMC Cancer* **11**, 106 (2011).

123. Zhang, H. *et al.* Hyaluronan-mediated motility receptor confers resistance to chemotherapy via TGFβ/Smad2-induced epithelial-mesenchymal transition in gastric cancer. *FASEB J* **33**, 6365–6377 (2019).

124. Maxwell, C. A. *et al.* Interplay between BRCA1 and RHAMM regulates epithelial apicobasal polarization and may influence risk of breast cancer. *PLoS Biol* **9**, e1001199 (2011).

125. Tarullo, S. E. *et al.* Receptor for Hyaluronan-Mediated Motility (RHAMM) defines an invasive niche associated with tumor progression and predicts poor outcomes in breast cancer patients. 2022.06.13.495375 Preprint at https://doi.org/10.1101/2022.06.13.495375 (2022).

126. Tolg, C. *et al.* RHAMM Promotes Interphase Microtubule Instability and Mitotic Spindle Integrity through MEK1/ERK1/2 Activity. *J Biol Chem* **285**, 26461–26474 (2010).

127. Telmer, P. G., Tolg, C., McCarthy, J. B. & Turley, E. A. How does a protein with dual mitotic spindle and extracellular matrix receptor functions affect tumor susceptibility and progression? *Commun Integr Biol* **4**, 182–185 (2011).

128. Casey, J. *et al.* 3D hydrogel-based microwell arrays as a tumor microenvironment model to study breast cancer growth. *Biomed. Mater.* **12**, 025009 (2017).

129. Imamura, Y. *et al.* Comparison of 2D- and 3D-culture models as drug-testing platforms in breast cancer. *Oncol Rep* **33**, 1837–1843 (2015).

130. Fisher, M. F. & Rao, S. S. Three-dimensional culture models to study drug resistance in breast cancer. *Biotechnol Bioeng* **117**, 2262–2278 (2020).

131. Edmondson, R., Broglie, J. J., Adcock, A. F. & Yang, L. Three-dimensional cell culture systems and their applications in drug discovery and cell-based biosensors. *Assay Drug Dev Technol* **12**, 207–218 (2014).

132. Eglen, R. M. & Klein, J.-L. Three-Dimensional Cell Culture: A Rapidly Emerging Approach to Cellular Science and Drug Discovery. *SLAS Discov* **22**, 453–455 (2017).

133. Chaicharoenaudomrung, N., Kunhorm, P. & Noisa, P. Three-dimensional cell culture systems as an in vitro platform for cancer and stem cell modeling. *World J Stem Cells* **11**, 1065–1083 (2019).

134. Breslin, S. & O'Driscoll, L. The relevance of using 3D cell cultures, in addition to 2D monolayer cultures, when evaluating breast cancer drug sensitivity and resistance. *Oncotarget* **7**, 45745–45756 (2016).

135. Weaver, V. M. *et al.* beta4 integrin-dependent formation of polarized three-dimensional architecture confers resistance to apoptosis in normal and malignant mammary epithelium. *Cancer Cell* **2**, 205–216 (2002).

136. Li, Q., Chow, A. B. & Mattingly, R. R. Three-dimensional overlay culture models of human breast cancer reveal a critical sensitivity to mitogen-activated protein kinase kinase inhibitors. *J Pharmacol Exp Ther* **332**, 821–828 (2010).

137. Cailleau, R., Young, R., Olivé, M. & Reeves, W. J. Breast tumor cell lines from pleural effusions. *J Natl Cancer Inst* **53**, 661–674 (1974).

138. Minn, A. J. *et al.* Genes that mediate breast cancer metastasis to lung. *Nature* **436**, 518–524 (2005).

139. Prat, A. & Perou, C. M. Deconstructing the molecular portraits of breast cancer. *Mol Oncol* **5**, 5–23 (2011).

140. Chavez, K. J., Garimella, S. V. & Lipkowitz, S. Triple Negative Breast Cancer Cell Lines: One Tool in the Search for Better Treatment of Triple Negative Breast Cancer. *Breast Dis* **32**, 35–48 (2010).

141. Prat, A. *et al.* Phenotypic and molecular characterization of the claudin-low intrinsic subtype of breast cancer. *Breast Cancer Research* **12**, R68 (2010).

142. Demidenko, E. & Miller, T. W. Statistical determination of synergy based on Bliss definition of drugs independence. *PLOS ONE* **14**, e0224137 (2019).

143. Messam, B. J., Tolg, C., McCarthy, J. B., Nelson, A. C. & Turley, E. A. RHAMM Is a Multifunctional Protein That Regulates Cancer Progression. *Int J Mol Sci* **22**, 10313 (2021).

144. Kapałczyńska, M. *et al.* 2D and 3D cell cultures – a comparison of different types of cancer cell cultures. *Arch Med Sci* **14**, 910–919 (2018).

145. Jensen, C. & Teng, Y. Is It Time to Start Transitioning From 2D to 3D Cell Culture? *Frontiers in Molecular Biosciences* **7**, (2020).

146. Lee, G. Y., Kenny, P. A., Lee, E. H. & Bissell, M. J. Three-dimensional culture models of normal and malignant breast epithelial cells. *Nat Methods* **4**, 359–365 (2007).

147. Muguruma, M. *et al.* Differences in drug sensitivity between two-dimensional and three-dimensional culture systems in triple-negative breast cancer cell lines. *Biochemical and Biophysical Research Communications* **533**, 268–274 (2020).

148. Kim, S.-Y. *et al.* Doxorubicin-induced reactive oxygen species generation and intracellular Ca2+increase are reciprocally modulated in rat cardiomyocytes. *Exp Mol Med* **38**, 535–545 (2006).

149. Pommier, Y., Leo, E., Zhang, H. & Marchand, C. DNA Topoisomerases and Their Poisoning by Anticancer and Antibacterial Drugs. *Chemistry & Biology* **17**, 421–433 (2010).

150. Lim, P. T., Goh, B. H. & Lee, W.-L. 3 - Taxol: Mechanisms of action against cancer, an update with current research. in *Paclitaxel* (eds. Swamy, M. K., Pullaiah, T. & Chen, Z.-S.) 47–71 (Academic Press, 2022). doi:10.1016/B978-0-323-90951-8.00007-2.

151. Zhou, Q. *et al.* Genes That Predict Poor Prognosis in Breast Cancer via Bioinformatical Analysis. *Biomed Res Int* **2021**, 6649660 (2021).

152. Tolg, C., Poon, R., Fodde, R., Turley, E. A. & Alman, B. A. Genetic deletion of receptor for hyaluronan-mediated motility (Rhamm) attenuates the formation of aggressive fibromatosis (desmoid tumor). *Oncogene* **22**, 6873–6882 (2003).

153. Tolg, C., Messam, B. J.-A., McCarthy, J. B., Nelson, A. C. & Turley, E. A. Hyaluronan Functions in Wound Repair That Are Captured to Fuel Breast Cancer Progression. *Biomolecules* **11**, 1551 (2021).

154.   Koelzer, V. H. *et al.* Expression of the hyaluronan-mediated motility receptor RHAMM in tumor budding cells identifies aggressive colorectal cancers. *Hum Pathol* **46**, 1573–1581 (2015).

155.   Lugowska, I., Koseła-Paterczyk, H., Kozak, K. & Rutkowski, P. Trametinib: a MEK inhibitor for management of metastatic melanoma. *Onco Targets Ther* **8**, 2251–2259 (2015).

156.   Research, C. for D. E. and. FDA grants accelerated approval to dabrafenib in combination with trametinib for unresectable or metastatic solid tumors with BRAF V600E mutation. *FDA* (2022).

157.   Guo, Y.-J. *et al.* ERK/MAPK signalling pathway and tumorigenesis. *Exp Ther Med* **19**, 1997–2007 (2020).

158.   Tolcher, A. W. *et al.* Phase I dose-escalation trial of the oral AKT inhibitor uprosertib in combination with the oral MEK1/MEK2 inhibitor trametinib in patients with solid tumors. *Cancer Chemother Pharmacol* **85**, 673–683 (2020).

159.   Hauser-Kawaguchi, A., Luyt, L. G. & Turley, E. Design of peptide mimetics to block pro-inflammatory functions of HA fragments. *Matrix Biol* **78–79**, 346–356 (2019).

160.   Lehár, J. *et al.* Synergistic drug combinations tend to improve therapeutically relevant selectivity. *Nat Biotechnol* **27**, 659–666 (2009).

161.   Cocco, S. *et al.* Biomarkers in Triple-Negative Breast Cancer: State-of-the-Art and Future Perspectives. *Int J Mol Sci* **21**, 4579 (2020).

162.   Otto, T. & Sicinski, P. Cell cycle proteins as promising targets in cancer therapy. *Nat Rev Cancer* **17**, 93–115 (2017).

163.   Sohr, S. & Engeland, K. RHAMM is differentially expressed in the cell cycle and downregulated by the tumor suppressor p53. *Cell Cycle* **7**, 3448–3460 (2008).

164.   Chen, H. *et al.* Spatial regulation of Aurora A activity during mitotic spindle assembly requires RHAMM to correctly localize TPX2. *Cell Cycle* **13**, 2248–2261 (2014).

165.   Mohapatra, S., Yang, X., Wright, J. A., Turley, E. A. & Greenberg, A. H. Soluble hyaluronan receptor RHAMM induces mitotic arrest by suppressing Cdc2 and cyclin B1 expression. *J Exp Med* **183**, 1663–1668 (1996).

166.   Vakili, T. An invasive tumor cell subpopulation as a therapeutic target in breast cancer. *Electronic Thesis and Dissertation Repository* (2017).

167.   Scholzen, T. & Gerdes, J. The Ki-67 protein: From the known and the unknown. *Journal of Cellular Physiology* **182**, 311–322 (2000).

168.   van der Vaart, B., Akhmanova, A. & Straube, A. Regulation of microtubule dynamic instability. *Biochem Soc Trans* **37**, 1007–1013 (2009).

169.   Forth, S. & Kapoor, T. M. The mechanics of microtubule networks in cell division. *Journal of Cell Biology* **216**, 1525–1531 (2017).

170.   Roberts, P. J. & Der, C. J. Targeting the Raf-MEK-ERK mitogen-activated protein kinase cascade for the treatment of cancer. *Oncogene* **26**, 3291–3310 (2007).

171.   Hatano, H. *et al.* Overexpression of receptor for hyaluronan-mediated motility (RHAMM) in MC3T3-E1 cells induces proliferation and differentiation through phosphorylation of ERK1/2. *J Bone Miner Metab* **30**, 293–303 (2012).

172.   Yoon, S. & Seger, R. The extracellular signal-regulated kinase: Multiple substrates regulate diverse cellular functions. *Growth Factors* **24**, 21–44 (2006).

173.   Ramos, J. W. The regulation of extracellular signal-regulated kinase (ERK) in mammalian cells. *Int J Biochem Cell Biol* **40**, 2707–2719 (2008).

174.   Hardwick, C. *et al.* Molecular cloning of a novel hyaluronan receptor that mediates tumor cell motility. *J Cell Biol* **117**, 1343–1350 (1992).

175.   Entwistle, J. *et al.* Characterization of the murine gene encoding the hyaluronan receptor RHAMM. *Gene* **163**, 233–238 (1995).

176.   Hall, C. L. *et al.* Overexpression of the hyaluronan receptor RHAMM is transforming and is also required for H-ras transformation. *Cell* **82**, 19–26 (1995).

177.   Tolg, C. *et al.* Cell-specific expression of the transcriptional regulator RHAMM provides a timing mechanism that controls appropriate wound re-epithelialization. *J Biol Chem* **295**, 5427–5448 (2020).

178.   Song, J. M. *et al.* Hyaluronan-CD44/RHAMM interaction-dependent cell proliferation and survival in lung cancer cells. *Molecular Carcinogenesis* **58**, 321–333 (2019).

179.   Aitken, K. & Bägl, D. J. Stretch-induced bladder smooth muscle cell (SMC) proliferation is mediated by RHAMM-dependent extracellular-regulated kinase (erk) signaling. *Urology* **57**, 109 (2001).

180.   Lompardía, S. L., Papademetrio, D. L., Mascaró, M., Álvarez, E. M. del C. & Hajos, S. E. Human leukemic cell lines synthesize hyaluronan to avoid senescence and resist chemotherapy. *Glycobiology* **23**, 1463–1476 (2013).

181.   Horwitz, S. B. Taxol (paclitaxel): mechanisms of action. *Ann Oncol* **5 Suppl 6**, S3-6 (1994).

182.   Tarr, M. & van Helden, P. D. Inhibition of transcription by adriamycin is a consequence of the loss of negative superhelicity in DNA mediated by topoisomerase II. *Mol Cell Biochem* **93**, 141–146 (1990).

183. Han, J. *et al.* Chemoresistance in the Human Triple-Negative Breast Cancer Cell Line MDA-MB-231 Induced by Doxorubicin Gradient Is Associated with Epigenetic Alterations in Histone Deacetylase. *Journal of Oncology* **2019**, e1345026 (2019).

184. Chen, D.-R., Lu, D.-Y., Lin, H.-Y. & Yeh, W.-L. Mesenchymal Stem Cell-Induced Doxorubicin Resistance in Triple Negative Breast Cancer. *Biomed Res Int* **2014**, 532161 (2014).

185. Paramanantham, A. *et al.* Doxorubicin-Resistant TNBC Cells Exhibit Rapid Growth with Cancer Stem Cell-like Properties and EMT Phenotype, Which Can Be Transferred to Parental Cells through Autocrine Signaling. *Int J Mol Sci* **22**, 12438 (2021).

186. Tacar, O., Sriamornsak, P. & Dass, C. R. Doxorubicin: an update on anticancer molecular action, toxicity and novel drug delivery systems. *J Pharm Pharmacol* **65**, 157–170 (2013).

187. Gewirtz, D. A critical evaluation of the mechanisms of action proposed for the antitumor effects of the anthracycline antibiotics adriamycin and daunorubicin. *Biochemical Pharmacology* **57**, 727–741 (1999).

188. Chen, N.-T. *et al.* Probing the Dynamics of Doxorubicin-DNA Intercalation during the Initial Activation of Apoptosis by Fluorescence Lifetime Imaging Microscopy (FLIM). *PLOS ONE* **7**, e44947 (2012).

189. Dai, J. *et al.* Elimination of quiescent slow-cycling cells via reducing quiescence depth by natural compounds purified from Ganoderma lucidum. *Oncotarget* **8**, 13770–13781 (2017).

190. Niedworok, C. *et al.* The Impact of the Receptor of Hyaluronan-Mediated Motility (RHAMM) on Human Urothelial Transitional Cell Cancer of the Bladder. *PLoS One* **8**, e75681 (2013).

191. Wang, Z. *et al.* Interplay of mevalonate and Hippo pathways regulates RHAMM transcription via YAP to modulate breast cancer cell motility. *Proc Natl Acad Sci U S A* **111**, E89–E98 (2014).

192. Zhou, J.-N., Ljungdahl, S., Shoshan, M. C., Swedenborg, J. & Linder, S. Activation of tissue-factor gene expression in breast carcinoma cells by stimulation of the RAF-ERK signaling pathway. *Molecular Carcinogenesis* **21**, 234–243 (1998).

193. Leung, E. Y. *et al.* Relationships between Signaling Pathway Usage and Sensitivity to a Pathway Inhibitor: Examination of Trametinib Responses in Cultured Breast Cancer Lines. *PLOS ONE* **9**, e105792 (2014).

194. Liu, F., Yang, X., Geng, M. & Huang, M. Targeting ERK, an Achilles' Heel of the MAPK pathway, in cancer therapy. *Acta Pharmaceutica Sinica B* **8**, 552–562 (2018).

195. Cargnello, M. & Roux, P. P. Activation and Function of the MAPKs and Their Substrates, the MAPK-Activated Protein Kinases. *Microbiol Mol Biol Rev* **75**, 50–83 (2011).

196. Gershenson, D. M. *et al.* Trametinib versus standard of care in patients with recurrent low-grade serous ovarian cancer (GOG 281/LOGS): an international, randomised, open-label, multicentre, phase 2/3 trial. *The Lancet* **399**, 541–553 (2022).

197. Carvalho, A. M., Soares da Costa, D., Reis, R. L. & Pashkuleva, I. RHAMM expression tunes the response of breast cancer cell lines to hyaluronan. *Acta Biomaterialia* **146**, 187–196 (2022).

198. Santini, C. C. *et al.* Global view of the RAF-MEK-ERK module and its immediate downstream effectors. *Sci Rep* **9**, 10865 (2019).

199. Gu, J. *et al.* MEK or ERK inhibition effectively abrogates emergence of acquired osimertinib resistance in the treatment of epidermal growth factor receptor-mutant lung cancers. *Cancer* **126**, 3788–3799 (2020).

200. Landry, I., Sumbly, V. & Vest, M. Advancements in the Treatment of Triple-Negative Breast Cancer: A Narrative Review of the Literature. *Cureus* **14**, e21970 (2022).

201. Schwaederle, M. *et al.* Impact of Precision Medicine in Diverse Cancers: A Meta-Analysis of Phase II Clinical Trials. *J Clin Oncol* **33**, 3817–3825 (2015).

202. Tsimberidou, A.-M. *et al.* Personalized medicine for patients with advanced cancer in the phase I program at MD Anderson: validation and landmark analyses. *Clin Cancer Res* **20**, 4827–4836 (2014).

203. Hanahan, D. Hallmarks of Cancer: New Dimensions. *Cancer Discovery* **12**, 31–46 (2022).

204. Nowak-Sliwinska, P. *et al.* Optimization of drug combinations using Feedback System Control. *Nat Protoc* **11**, 302–315 (2016).

205. Vogus, D. R., Pusuluri, A., Chen, R. & Mitragotri, S. Schedule dependent synergy of gemcitabine and doxorubicin: Improvement of in vitro efficacy and lack of in vitro-in vivo correlation. *Bioeng Transl Med* **3**, 49–57 (2018).

206. Christowitz, C. *et al.* Mechanisms of doxorubicin-induced drug resistance and drug resistant tumour growth in a murine breast tumour model. *BMC Cancer* **19**, 757 (2019).

207. Abrams, S. L. *et al.* The Raf/MEK/ERK pathway can govern drug resistance, apoptosis and sensitivity to targeted therapy. *Cell Cycle* **9**, 1781–1791 (2010).

208. Chang, F. *et al.* Involvement of PI3K/Akt pathway in cell cycle progression, apoptosis, and neoplastic transformation: a target for cancer chemotherapy. *Leukemia* **17**, 590–603 (2003).

209. West, K. A., Sianna Castillo, S. & Dennis, P. A. Activation of the PI3K/Akt pathway and chemotherapeutic resistance. *Drug Resistance Updates* **5**, 234–248 (2002).

210. Qiu, J.-G. *et al.* Trametinib modulates cancer multidrug resistance by targeting ABCB1 transporter. *Oncotarget* **6**, 15494–15509 (2015).

211. Huang, S. *et al.* Dextran methacrylate hydrogel microneedles loaded with doxorubicin and trametinib for continuous transdermal administration of melanoma. *Carbohydrate Polymers* **246**, 116650 (2020).

212. Sherman, E. J. *et al.* A pilot study of trametinib in combination with paclitaxel in the treatment of anaplastic thyroid cancer. *JCO* **40**, 6088–6088 (2022).

213. Awasthi, N., Monahan, S., Stefaniak, A., Schwarz, M. A. & Schwarz, R. E. Inhibition of the MEK/ERK pathway augments nab-paclitaxel-based chemotherapy effects in preclinical models of pancreatic cancer. *Oncotarget* **9**, 5274–5286 (2017).

214. Demidenko, Z. N. *et al.* Mechanism of G1-like arrest by low concentrations of paclitaxel: next cell cycle p53-dependent arrest with sub G1 DNA content mediated by prolonged mitosis. *Oncogene* **27**, 4402–4410 (2008).

215. Watanabe, M., Sowa, Y., Yogosawa, M. & Sakai, T. Novel MEK inhibitor trametinib and other retinoblastoma gene (RB)-reactivating agents enhance efficacy of 5-fluorouracil on human colon cancer cells. *Cancer Science* **104**, 687–693 (2013).

216. Joshi, M., Rice, S. J., Liu, X., Miller, B. & Belani, C. P. Trametinib with or without Vemurafenib in BRAF Mutated Non-Small Cell Lung Cancer. *PLOS ONE* **10**, e0118210 (2015).

217. Schick, U. *et al.* Trametinib radiosensitises RAS- and BRAF-mutated melanoma by perturbing cell cycle and inducing senescence. *Radiother Oncol* **117**, 364–375 (2015).

218. Bar-On, O., Shapira, M. & Hershko, D. D. Differential effects of doxorubicin treatment on cell cycle arrest and Skp2 expression in breast cancer cells. *Anticancer Drugs* **18**, 1113–1121 (2007).

219. Cromwell, E. F. *et al.* Multifunctional profiling of triple-negative breast cancer patient-derived tumoroids for disease modeling. *SLAS Discov* **27**, 191–200 (2022).

Curriculum Vitae

Britney Messam

Education

09/2020 – 08/2022	**Master of Science,** *Biochemistry* Western University, London, Ontario
09/2016 – 04/2020	**Bachelor of Medical Science,** *Honours Specialization in Biochemistry and Cell Biology* Western University, London, Ontario

Awards and Distinctions

09/2021 – 08/2022	**Dean's Research Scholarship** ($10,000) *Western University*
09/2021 – 08/2022	**MSc. Translational Breast Cancer Research Studentship** ($10,000) - Declined *Western University*
09/2020 – 08/2021	**MSc. Translational Breast Cancer Research Studentship** ($17,000) *Western University*
05/2019 – 08/2019	**NSERC Undergraduate Student Research Award** ($6,500) *Ontario Tech University*
09/2017 – 04/2020	**Dean's Honor List** *Western University*
09/2016 – 04/2017	**Western Scholarship of Distinction** ($1,000) *Western University*

Related Work Experience

09/2021 – 12/2021	**Graduate Teaching Assistant,** *Department of Biochemistry* Western University, London, Ontario ▪ Provided critical feedback on over 50 undergraduate students' infographics spanning a variety of biochemistry topics ▪ Supervised large groups of students during examination periods

Publications

1. **Messam, B.J.;** Tolg, C.; McCarthy, J.B.; Nelson, A.C.; Turley, E.A. RHAMM Is a Multifunctional Protein That Regulates Cancer Progression. Int. J. Mol. Sci. 2021, 22, 10313. https://doi.org/10.3390/ijms221910313
2. Tolg, C.; **Messam, B.J.-A**.; McCarthy, J.; Nelson, A.C.; Turley, E.A. Hyaluronan Functions in Wound Repair That Are Captured to Fuel Breast Cancer Progression. Biomolecules **2021**, 11, 1551. https://doi.org/10.3390/biom11111551